İSTANBUL TECHNICAL UNIVERSITY ★ INSTITUTE OF SCIENCE AND TECHNOLOGY

REPASSIVATION/DEPASSIVATION KINETICS OF 316L STAINLESS STEEL IN RECIPROCATING SLIDING CONTACTS

M.Sc. Thesis by

Gökhan BÜYÜKSARI, B.Sc.

Department : Metallurgical and Materials Engineering

Programme : Materials Engineering

JUNE 2008

İSTANBUL TECHNICAL UNIVERSITY ★ INSTITUTE OF SCIENCE AND TECHNOLOGY

REPASSIVATION/DEPASSIVATION KINETICS OF 316L STAINLESS STEEL IN RECIPROCATING SLIDING CONTACTS

M.Sc. Thesis by
Gökhan BÜYÜKSARI, B.Sc.
(506061406)

Date of submission : 5 May 2008

Date of defence examination: 9 June 2008

Supervisor (Chairman): Prof. Dr. Hüseyin ÇİMENOĞLU

Members of the Examining Committee Prof.Dr. Eyüp Sabri KAYALI

Prof.Dr. Mehmet KOZ (MÜ)

JUNE 2008

İSTANBUL TEKNİK ÜNİVERSİTESİ ★ FEN BİLİMLERİ ENSTİTÜSÜ

316L PASLANMAZ ÇELİĞİNİN KARŞI YÜKLEMELİ AŞINMA KOŞULLARI ALTINDAKİ REPASİVASYON/DEPASİVASYON KİNETİĞİ

YÜKSEK LİSANS TEZİ

Müh. Gökhan BÜYÜKSARI

(506061406)

Tezin Enstitüye Verildiği Tarih : 5 Mayıs 2008

Tez Danışmanı : **Prof. Dr. Hüseyin ÇİMENOĞLU**

Diğer Jüri Üyeleri **Prof. Dr. Eyüp Sabri KAYALI**

Prof. Dr. Mehmet KOZ (M.Ü.)

HAZİRAN 2008

ACKNOWLEDGEMENTS

First of all I would like express my sincere gratitudes to my family whom I care about more than anything, for their invaluable support and love.

I would like to thank to my advisor Prof. Dr. Hüseyin Çimenoğlu for his unique guidance. It's always been a pleasure from my side being a master student in his research group. Above all, I would like to thank him additionally for his kind attitude as personally.I also would like to thank to Assistant Prof. Murat Baydoğan for his guidance, help and positive attitude.

My special thanks are for Prof. Dr. Jean Pierre Celis, head of the research group on Surface Engineering and Tribology at Kath. Uni. Leuven in Belgium, for giving me the opportunity of working in his research group as an exchange student during the first semester of 2nd year of my master. In addition to being very excellent professor, he has been also very kind personally. I couldn't have completed my master dissertation without his encouragement and guidance. I also want to thank to the MTM department of K.U. Leuven, especially Marc Peeters who was responsible engineer of the tribology laboratory in that department, for helping me during the laboratory work. And I would like to thank to Iacomi Marius Adrian who was working together with me at the MTM tribology laboratory, for his great friendship.

I would like to thank to my colleague Fatih Uysal who is also very close friend of mine from the beginning of the university career, for his help on my experimental work. I would like to forward my thankfullness to my valuable friend Metallurgy Engineer Ferhat Omaç for his unforgettable friendship and contribution on preparing master dissertation.

I would like to forward my thanks to the department of Metallurgical and Materials Engineering of Istanbul Technical University providing very valuable two years of education.

May, 2008 Gökhan BÜYÜKSARI

CONTENTS

ACKNOWLEDGEMENTS **I**
ABBREVIATIONS **IV**
LIST OF TABLES **V**
LIST OF FIGURES **VI**
LIST OF SYMBOLS **VII**
ÖZET **VIII**
SUMMARY **IX**

1. INTRODUCTION **1**

2. FRICTION IN VIBRATING CONTACTS **3**

2.1. Phenomena of Dry Friction **3**

2.2. Fretting Concept **4**

2.2.1. Model contact and contact pressure 6
2.2.2. Contact exposure 7

3. TRIBOCORROSION **9**

3.1. Tribocorrosion Phenomena Definition **9**

3.2. Parameters Affecting The Tribocorrosion System **11**

3.2.1. Repassivation Kinetics 12

4. EXPERIMENTAL **14**

4.1. Materials and Method **14**

4.2. Characterization Work **17**

5. RESULTS **18**

5.1. Friction and Wear Results **18**

5.2. Profilometric Analyses Results **21**

5.3. Scanning Electron Microscope (SEM) Analyses Results **24**

5.4. Orientation Image Microscopy (OIM) Analyses Results **28**

6. DISCUSSION **30**

7. CONCLUSIONS **32**

REFERENCES **34**

APPENDIX A **38**

BIOGRAPHY **41**

ABBREVIATIONS

MUST	**:** Modular Universal Surface Tester
RH	**:** Relative Humidity
SS	**:** Stainless Steel
SEM	**:** Scanning Electron Microscopy
OIM	**:** Orientation Image Microscopy
AFM	**:** Atomic Force Microscopy

LIST OF TABLES

Page No

Table 4.1 Fretting test parameters 16

LIST OF FIGURES

Page No

Figure 2.1 : Aspects of dry friction 3
Figure 2.2 : Schematic representation of the basic fretting modes and displacement trajectories defined for the circular contact periphery of a ball-on-flat model contact 5
Figure 2.3 : Characteristic hysteresis loops between the tangential force and the fretting displacement representing 6
Figure 2.4 : Exposure time at different positions in the fretting zone..... 8
Figure 3.1 : Parameters that affect the tribocorrosion system of a sliding contact affect the tribocorrosion behavior of a sliding contact..... 12
Figure 4.1 : Falex Tribology MUST tester..... 14
Figure 4.2 : MUST microtribometer and its components 15
Figure 5.1 : Evolution of tangential force throughout fretting period for test performed at varying holding times 19
Figure 5.2 : Variation of the coefficient of friction as a function of number of cycles recorded during fretting tests 20
Figure 5.3: 3D profilometric surface topography of the fretting scars on 316L stainless steel obtained at different holding times in ambient air test conditions..... 22
Figure 5.4 : 3D surface topography of the fretting scars after smoothing treatment 23
Figure 5.5 : Variation of the depth of wear scars on 316L stainless steel obtained after fretting tests done at different holding times in ambient air of 50% RH 24
Figure 5.6 : SEM images of fretting scars..... 26
Figure 5.7 : SEM of fretting scar obtained by the intermittent fretting test with holding time of 8 s and its zoom in view..... 27
Figure 5.8 : Orientation Image Microscopy (OIM) scans of the fretting scars 29
Figure 6.1 : Variation of coefficient of friction as a function of holding time for fretting tests performed on 316L stainless steel sliding against corundum balls in ambient air of 50% RH. 31
Figure A.1 : Figure A.2 SEM of fretting scar obtained by the continuous fretting test and its zoom in view..... 38
Figure A.2 : SEM of fretting scar obtained by the intermittent fretting test with holding time of 0.5 s and its zoom in view..... 39
Figure A.3 : SEM of fretting scar obtained by the intermittent fretting test with holding time of 10 s and its zoom in view..... 40

LIST OF SYMBOLS

$\mathbf{a}$	: Hertzian contact radius
$\mathbf{d}$	: Distance
$\mathbf{E, E^*}$	: Young's modulus and effective Young's modulus
$\mathbf{E_d}$	: Dissipated energy
$\mathbf{F_f}$	: Friction force
$\boldsymbol{f}$	: Frequency
$\mathbf{F_n}$,$\mathbf{F'_n}$	: Normal force and relative normal force
$\mathbf{F_{t,dyn}}$	: Dynamic tangential force
$\mathbf{F_t, F_{t,max}}$	: Tangential forceand maximum tangential force
$\mathbf{K_t, K_n}$	: Tangential stiffness and normal stiffness
$\boldsymbol{\mu}$	: Coefficient of friction
$\boldsymbol{\mu_s, \mu_d}$	: Static coefficient of friction and dynamic coefficient of friction
$\mathbf{R_a}$	: Average roughness
$\mathbf{r}$	: Radius
$\mathbf{p}$	: Contact pressure
$\boldsymbol{\upsilon}$	: Poisson's ratio
$\mathbf{t_{max}, t_{min}}$	: Maximum time and minimum time

316L PASLANMAZ ÇELİĞİNİN KARŞI YÜKLEMELİ AŞINMA KOŞULLARI ALTINDAKİ REPASİVASYON/DEPASİVASYON KİNETİĞİ

ÖZET

Tribolojik sistemlerin birçoğunda, tribolojik kontağı meydana getiren malzemeler, hem mekanik hem de kimyasal etkileşimlere maruz kalmaktadırlar. Bu koşullar altında tribolojik kontağın aşınmasını, korozyonu ihmal ederek basitçe aşınma direnci bilgisinden veya sürtünmeyi ihmal ederek korozyon dayanımına bağlı bir tahmin yapmak mümkün değildir.

Paslanmaz çelikler agresif ve korozif çevre etkenlerine karşı yüzeylerinde oluşturdukları nanometre mertebesindeki pasif oksit filmi sayesinde kendilerini korurlar. Bu oksit filmi ortamda oksijen bulunduğu müddetçe kendini daima yenileyebilir ancak abrazif bir etki sonucunda bu film lokal olarak bozunabilir veya tamamen sistemden kaldırılabilir. Bu olayı, malzemenin maruz kaldığı çevre koşullarına ve yükleme koşullarına bağlı olarak malzemenin lokal olarak aşınması veya o bölgenin tekrar pasif konuma geçmesi takip eder. Repasivasyon kinetiği bu tür pasif malzemelerin korozyon-aşınma davranışını kritik olarak etkiler.

Bu çalışmada, 316L paslanmaz çeliğine, aktif aşınma bölgesinin çevre koşullarıyla etkileşme süresine bağlı olarak ileri-geri, karşı yüklemeli aşınma testleri uygulandı. Çalışmada, her karşı yüklemeli çevrimden sonra tutma zamanı uygulama ve istenilen pozisyonda, istenilen süre zarfında tutma olanağı sağlayan ve bu sayede çevre koşullarına maruz kalma süresini kontrol edebilme olanağı sunan özel bir mikro aşındırma test düzeneği kullanıldı. Farklı sürelerde, çok sayıda test uygulanarak, sürtünme katsayısı ve aşınma gelişimi analiz edildi ve tribolojik kontağın etkisine bağlı olarak 316L paslanmaz çeliğinin sürtünme koşulları altındaki aşınma davranışı incelendi.

REPASSIVATION/DEPASSIVATION KINETICS OF 316L STAINLESS STEEL IN RECIPROCATING SLIDING CONTACS

SUMMARY

In many tribological systems, the materials forming the tribological contact are exposed to a corrosive environment and therefore they are subjected to both mechanical and chemical solicitations. Under these conditions the rate of degredation of a tribological contact cannot be predicted simply from knowledge of the wear resistanse in the absance of corrosion or from the corrosion resistance in the absance of friction.

Stainless steels rely on a nanometer degree thick surface oxide passive film for their protection from aggressive and corrosive environments. This oxide film forms instantaneously when oxygen is available in the environment but abrasion can lead to the local rupture or complete removal of these films. This can be followed by a local dissolution or repassivation of the active metal depending on the material-electrolyte system and the loading conditions. The kinetics of repassivation critically affects the corrosion wear of such passive materials.

In this work, 316L stainless steel was subjected to reciprocating bidirectional (fretting) sliding with varying exposure time of the active wear track to the environment. A special experimental set-up was used which allows to control the exposure time by a holding time applying after each reciprocating cycle and keep the reciprocating table at a fixed position for a selected time duration during the fretting tests. Performing large number of tests, evolution of coefficient of friction and the extent of wear was analysed with varying exposure time.In this approach, repassivation rate of 316L stainless steel was indicated. Degredation mechanism of 316L in reciprocating sliding contacts were analysed depending on the role of the contact.

1. INTRODUCTION

In tribological contacts operating in corrosive environments (tribocorrosion systems), material removal takes place simultaneously by mechanical wear and by corrosion.The two degradation mechanisms do not proceed independently, but mechanical and chemical phenomena interact with each other. For example, stainless steels are protected by a thin (1–10 nm thick) passive oxide film, which forms on the surface by spontaneous reaction with the environment. This oxide film forms instantaneously when oxygen is available in the environment but abrasion may lead to the local depassivation of the surface and cause local rupture or complete removal ov the passive film. This can lead to areas of the substrate being exposed to the environment and unless repassivation mechanism reform the passive film, accelerated dissolution will occur within these sites [1,2,3].

Generally, passive materials reacting with a corrosive environment exhibit an active–passive behaviour [4]. In such systems, corrosion and wear interactions are of great importance since the growth of an oxide film provides protection against corrosion while wear may break up and remove that oxide film. Thus, depending on film properties (stability, adherence, etc.) and repassivation kinetics, corrosion and wear interactions in these systems may accelerate the material loss. It is generally believed that rupture and removal of an oxide film from the surface lead to the exposure of active metal to the environment. This can be followed by a local dissolution or repassivation of the active metal depending on the material-electrolyte system and the loading conditions [5]. The kinetics of repassivation critically affects the corrosion wear of such passive materials [6]. Under these conditions the rate of degredation of a tribological contact cannot be predicted simply from knowledge of the wear resistance in the absance of corrosion or from the corrosion resistance in the absence of friction [7].

Depassivation-repassivation phenomena of passive materials have been studied by electrochemists, corrosion scientists and tribologists using different approaches.

Electrochemists and corrosion scientists are mainly interested in the study of kinetics of repassivation of depassivated surfaces. Tribologists, on the other hand, are interested in how surface oxidation during rubbing affects the rate of mechanical wear, in other words how the repassivation during the rubbing affects the wear rate. The investigation of localized depassivation and repassivation phenomena is of significance in understanding wear-corrosion mechanisms as well as in reducing material loss. Depassivation-repassivation phenomena of passive metals have been studied under conditions of mechanical breakdown of passive films in uni and bi-directional pin-on disk sliding, scratching, guillotining and abrasion and straining. In addition, depassivation-repassivation phenomena have also been investigated by electrochemical depassivation, pulsed laser depassivation and microtribocorrosion electrochemical techniques [8].

In this work, degredation mechanism of 316L stainless steel was investigated under reciprocating sliding contacts. As a function of exposure time of the active wear track to the environment, evolution of fretting wear behavior of 316L stainless steel was analysed and the role of contact mode was stressed. Insight of the obtained coefficient of friction data after each fretting test, repassivation/depassivation behavior of 316L stainless steel and the kinetics of repassivation of of 316L stainless steel was analysed.

2. FRICTION IN VIBRATING CONTACTS

2.1 Phenomena of Dry Friction

When a solid is moved tangentially with respect to the surface of another solid that it touches, or when an attempt is made to produce such a motion, a resistance to that motion occurs which is called friction [9]. Sliding without any lubricant to the sliding interface is considered as dry friction. Figure 2.1a represents the balance of forces of a flat body loaded on top of a plane and subjected to a force acting parallel to the contact interface. Newton's first law requires a relative force F'_n compensating the applied normal force F_n at the contact interface. The applied tangential force F_t is balanced by the friction force F_f resisting the relative motion along at the contact interface and by acceleration of the body at the onset of motion [10].

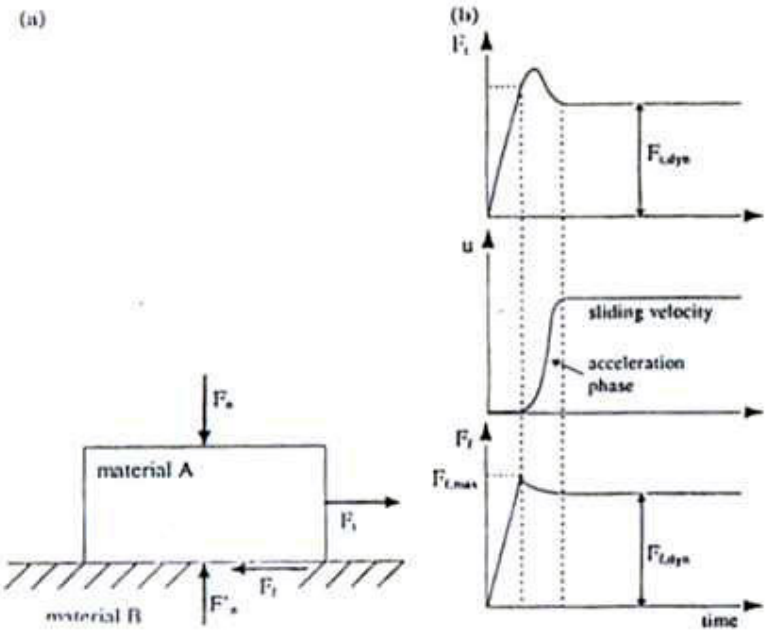

Figure 2.1: Aspects of dry friction (a)Equilibrium of forces on a flat-on-flat contact subjected to a normal force(F_n) and tangential (F_t) force.(b)Evolution of the tangential force, relative velocity, and friction force with time [10].

Increasing the applied tangential force continuously starting from zero results in a time evolution of the tangential force, the velocity of the body relative to the plane, and the friction force acting in the contact interface as schematically shown in Fig 2.1b Initially the applied tangential force increases linearly with time until a value of $F_{t,max}$ is reached. During this period, the relative velocity is zero, i.e., the body remains at rest. This phenomenon is called "static friction". Once F_t exceeds the value of $F_{t,max}$ the relative velocity along the contact interface increases from zero to a constant sliding phase during a short acceleration phase. The acceleration of the body mass requires a surplus in the applied tangential force. After a constant relative velocity is established, the tangential force drops to the constant value $F_{t,dyn}$. This phenomenon is known as "dynamic friction". Coulomb's experiments proved that the maximum static friction force at the onset of the motion is directly proportional to the normal force acting on the contact but does not depend on the size of the contact area. Therefore, the static coefficient of friction, μ_s, can be defined as the ratio [10].

$$\mu_s = \frac{F_{t,max}}{F_n} \quad \textbf{(2.1)}$$

This ratio is a constant for a given tribosystem. The tribosystem sticks under the condition that $F_t < \mu_s . F_n$ In the case of sliding, a constant friction force acts against the applied tangential force. Its value is also directly proportional to the applied normal force independent of the contact area so that the dynamic coefficient of friction, μ_d can be defined as [10],

$$\mu_d = \frac{F_{t,dyn}}{F_n} \quad \textbf{(2.2)}$$

In the case of sliding, the applied tangential force may be replaced by $\mu_d.F_n$ [10].

2.2 Fretting Concept

In the literature, the fretting is often defined as the action that produces fretting wear or fretting corrosion. The corrosive wear is usually called tribocorrosion which is the combined action of wear and corrosion process results in mutual interaction beyond their individual contribution. Tribocorrosion phenomenon is going to be described later [11].

When two surfaces in contact are subjected to an oscillatory movement of low amplitude, surface deterioration generally appears. The phenomena of wear induced by the term fretting, can develop in any mechanical device subjected to alternating movements such as vibrations or oscillations [11].

In several review papers, Waterhouse has pointed out a number of physical and chemical parameters affecting the appearance of fretting phenomena in vibrating contacts [12,13,14]. These are the contact geometry, type of vibration, contact normal force, the slip amplitude in the contact plane and contact environment (i.e., temperature, relative humidity, chemical composition)

The analysis of vibrating contacts in various practical applications indicated that fretting damage occurs at the relative displacements in the range of a few hundred nanometers to micrometers and the frequencies from about 0.1 to 10 kHz [12]. Additional information is required about the contact pressure and the test environment surrounding the vibrating contact. In the last two decades several research concepts for modelling contact vibrations have been established in order to relate the parameters of a simplified contact vibration to the mechanical and materials contact response. The mechanical response considers the distribution of slip, friction, tangential stress, and energy dissipationin the vibrating contact.The material response is reflected in the type of fretting damage, i.e., wear or cracking of the counterfaces as well as in chemical modifications of the mating materials and the detached debris.

Many industrial fretting situations can be conceptually reconstituted from a number of basic fretting modes. There are three basic modes as shown in Fig. 2.2.

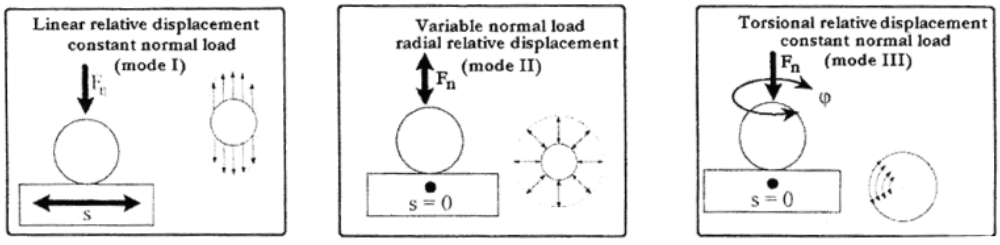

Figure 2.2: Schematic representation of the basic fretting modes and displacement trajectories defined for the circular contact periphery of a ball-on-flat model contact [10].

Most of the laboratory fretting experiments reported in literature have been performed under mode I. An oscillating linear displacement is imposed at constant frequency.

According to literature, two different cases are possible under fretting conditions, namely stick regime and gross slip regime :

1. Stick regime: $F_t<\mu_s F_n$. The applied tangential force, F_t, remains below the maximum friction force, F_n (μ_s is the static coefficient of friction). The relative velocity is zero at all positions in the contact zone, so that sticking is present over the entire contact area, as in Figure 2.3a. The fretting hysteresis loop is a straight line. When the tangential force is increased, the slip annulus expands reducing the diameter of the stick zone.

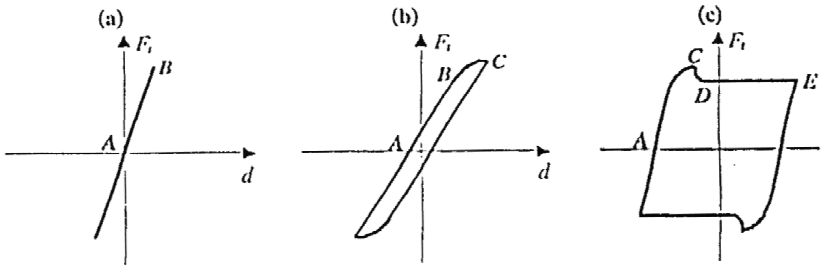

Figure 2.3: Characteristic hysteresis loops between the tangential force and the fretting displacement representing: a) elastic-stick, b) partial-slip and c) gross-slip fretting regime [10].

2. Gross-slip regime: $F_t>\mu_s F_n$. The applied tangential force exceeds the maximum friction force. Slip is established across the entire contact area regardless of the type of contact geometry. The loop area represents the frictional energy dissipated in the slips annulus [10].

2.2.1 Model contact and contact pressure

In fretting testing, variety of model contact geometries such as flat-on-flat, crossed cyclinders, and ball-on-flat configurations have been used.Due to the ease of contact alignment and the precise definition of the contact position in the test plane ball-on-flat configuration has particular advantage. The disadvantage of this model is that the contact area increases as wear occurs.This leads to a declining contact pressure if dead weight loading is applied.

In the case of a ball-on-flat model contact between isotropic, ideally elastic materials with perfect smooth surfaces, the contact area induced by the normal force F_n has a circular periphery with the Hertzian radius

$$a = \left(\frac{F_n}{E^*}\frac{3}{4}r\right)^{\frac{1}{3}} \qquad \text{where} \qquad \frac{1}{E^*} = \frac{1-\upsilon_1^2}{E_1} + \frac{1-\upsilon_1^2}{E_2} \tag{2.3}$$

Where r is the radius of the ball E and $\boldsymbol{\upsilon}$ are the Young's modulus and Poisson's ratio of the respective materials [12]. The ratio of the applied normal force to the induced contact area determines the avarage contact pressure.

$$p = \frac{F_n}{\pi a^2} \tag{2.4}$$

The contact pressure is not constant across the contact area but has a parabolic distribution along the diameter of the contact circle as

$$P(r) = \frac{3}{2}p\sqrt{1 - \left(\frac{r}{a}\right)^2} \tag{2.5}$$

with the maximum value

$$p_0 = \frac{3}{2}p \tag{2.6}$$

The contact centre (r=0). So the p_0 value calculated from the equation 2.4 gives the maximum Hertzian contact pressure of a given ball-on-flat contact [10].

2.2.2 Contact exposure

Contact exposure is an important aspect concerning the exchange of matter between the fretting zone and environment. During the exposure time, adsorption and chemical processes can take place as well as wear particles can escape from the contact. When the exposure time increases, triboreactions will be favored and the friction and wear will be influenced [15].

For the fretting conditions, contact exposure depends on the fretting mode, the location in the fretting zone, and the vibration parameters. In fretting mode III, none of the

contacting areas is exposed to the environment. In fretting mode II, the ring shaped slip zone on flat and the ball counterface is exposed to the test atmosphere.

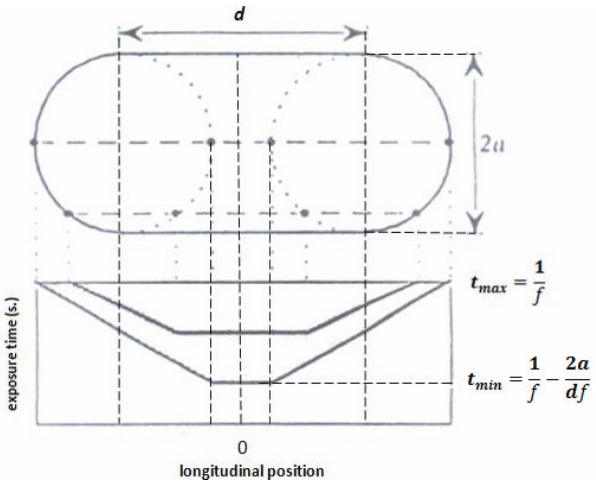

Figure 2.4: Exposure time at different positions in the fretting zone (d:displacement, f:frequnecy of the vibration, d:sliding distance, a:Hertzian contact radius)[8]

In fretting I, largest variation in the contact exposure is occurred. Each point in the contact zone on the flat will be exposed once the linear displacement stroke becomes larger than the Hertz diameter (Fig 2.4). The minimum contact exposure, t_{min} [8] is then determined by the contact radius, a, the linear sliding distance, d, and the vibration frequency, f as (d≥2a)

$$\boldsymbol{t_{min} = \frac{1}{f} - \frac{2a}{df}} \qquad \textbf{(2.7)}$$

An increased contact exposure at all points in the fretting zone can be achieved by reducing the vibration frequency. Part of the fretting zone is secluded from the environment when the sliding distance is reduced below the contact diameter. The counterface on the ball is not exposed directly to the environment throughout the vibration. The reduced contact exposure under fretting conditions can result in a friction and wear behavior which may significantly differ from that observed by other tribological testing methods. Two prominent effects contributing to these differences are incomplete tribochemical reactions with the environment and trapping of wear debris in the contact [10].

3. TRIBOCORROSION

3.1 Tribocorrosion Phenomena Definition

According to S. Mischler et al [16] tribocorrosion is a material degradation process which results from the combined effect of simultaneous mechanical wear and chemical (or electrochemical) material removal mechanisms. It is important to point out that the two mechanisms of degradation do not proceed separately, but depend on each other in a complex way: corrosion is accelerated by wear and, similarly wear may be affected by corrosion phenomena. Many aspects related to tribocorrosion mechanism are not yet fully understood, mostly due to the complexity of the chemical, electrochemical, physical and mechanical processes involved in a tribocorrosion system. Additionally, according to P. Ponthiaux [17], in practice field the tribocorrrosion occurrence is not yet recognized. Although the tribocorrosion topic is a very interesting and important subject, it is not widely written about.

Tribocorrosion phenomena have been studied for many years by electrochemists as well as by tribologists, using different approaches. Electrochemists and corrosion scientists are mainly interested in the study of kinetics of repassivation of depassivated surfaces. Tribologists, on the other hand, are interested in how surface oxidation during rubbing affects the rate of mechanical wear, in other words how the repassivation during the rubbing affects the wear rate. More recently, the mutual dependence of mechanical and electrochemical mechanisms has found increasing attention [8].

Electrochemical studies using mechanical abrasion were performed by several authors. Oltra et al. [18] used impinging particles to locally remove the passive film on iron for the study of repassivation kinetics. More recently Schmutz and Frankel [19] showed that local removal of passive films on aluminum alloys can be achieved using the AFM as a scratching device. Mentioned studies using mechanical abrasion and scratching for film removal were focused exclusively on the study of electrochemical phenomena related to

repassivation, but did not consider in detail the mechanical aspects of the contact. Generally, the mechanical parameters in these experiments were not well defined and no attempt was made to measure the extent of mechanical wear [7].

An overview of the classical theories of friction and wear including a description of the mechanism of oxidative wear has been given by Rabinowitz [20] and more recently by Lim and Ashby [21]. Oxidative wear has been identified as one of the four principal mechanisms of wear. Oxidative wear has been studied extensively by Quinn and coworkers [22]. According to their model chemical oxidation of the rubbing metal surfaces leads to growth of an oxide film, which periodically is eliminated from the contact due to the effect of mechanical forces. Stott [23] recently presented a review on the role of oxidation in wear with special consideration of high temperature systems. Fretting is a particular form of degradation observed in systems that are subjected to low amplitude vibrations. A wealth of experimental data on the role of corrosion under fretting conditions can be found in the book by Waterhouse [24]. The effect of corrosion on the wear rate in aqueous environments has been reviewed by Watson et al. [1] with special consideration to phenomena typically encountered in mining equipment. These authors describe the synergy effect between mechanical and chemical metal loss observed under tribocorrosion conditions. The mentioned wear studies in corrosive fluids were mostly carried out under open circuit conditions and the potential of the sliding metal (corrosion potential) was not measured.

A number of authors used electrochemical polarization to impose a fixed potential on the rubbing surfaces in order to study the effect of potential on the wear behavior. Brandon et al. [25] investigated the effect of an applied potential on the friction coefficient of mild steel in octanoic acid. Hong and Pyun [26] studied wear accelerated corrosion of 304 stainless steel in a pin-on-disk apparatus under external potential control. The measured total weight loss was compared to the weight loss observed in absence of rubbing. Iwabuchi et al. [27,28] used a reciprocating motion wear test apparatus including an alumina ball sliding on either 304 stainless steel or dye steel. The authors measured the anodic current resulting from rubbing and found that most of

the material removal was due to anodic dissolution rather than abrasion. Abd-el-Kader and El-Raghby [29,30] studied the wear behavior of stainless steel in chloride media at different applied potentials. The measured wear rate at potentials more negative than the corrosion potential was taken as a measure of mechanical wear and the difference between this value and the total wear rate observed at more anodic potentials was attributed to corrosion. The authors developed a theoretical model based on the assumption that the degradation proceeds by successive stages of build-up and removal of the passive oxide films. The effect of normal force or other mechanical aspects on this mechanism was not further considered. Xiaoxia et al. [31] observed that cathodic polarization of titanium led to increased wear due to hydrogen embrittlement. For this reason the rate of mechanical wear under anodic polarization is not necessarily equal that observed under cathodic polarization. Adler and Walters [32] proposed a model for tribocorrosion taking into account mechanical factors. These authors assumed that the extent of exposed bare metal surface in the wear scar is due to the plastic deformation of the metal and therefore depends on the applied normal force. The influence of electrode potential was not included in the model, however. More recently, Mischler et al. [33] proposed a model for the prediction of the rate of wear accelerated corrosion in a two body sliding contact taking into account both the effect of normal force and the repassivation behavior of the metal. The latter was characterized by the repassivation charge, which can be measured in an independent experiment and which is a function of the applied potential and of the material. Jemmely et al. [34] presented a model for the calculation of current transients measured in an electrochemically controlled electrochemical reciprocating motion tribometer taking into account film formation kinetics and ohmic effects.

3.2 Parameters Affecting The Tribocorrosion System

The tribocorrosion behavior of sliding contacts can be affected by many factors. However , the performance tribocorrosion systems is mainly conditioned by four types of parameters, namely: the mechanical solicitations which are related to equipment design and operation, the electrochemical conditions prevailing at the rubbing metal surfaces, the solution properties in the contact and the materials and surface properties of

the sample and the antagonist (Fig. 3.1). These parameters usually do not act independently, but their effects on the tribocorrosion behavior are mutually dependent [7].

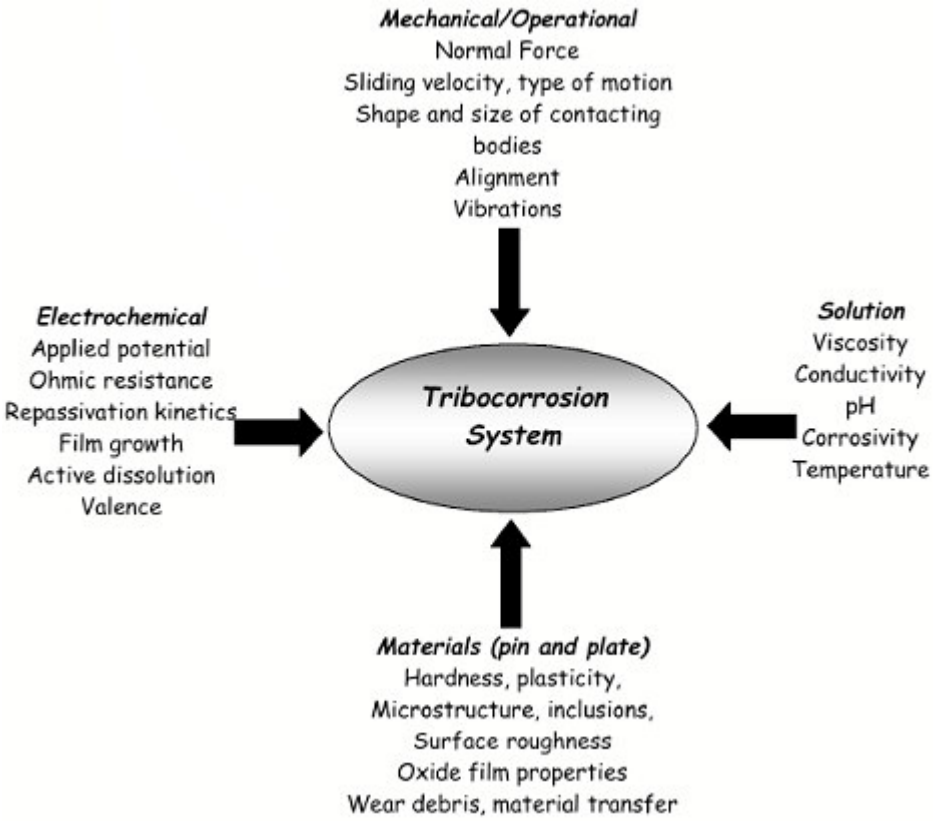

Figure 3.1: Parameters that affect the tribocorrosion system of a sliding contact affect the tribocorrosion behavior of a sliding contact [7].

3.2.1 Repassivation Kinetics

Passive materials under sliding conditions mainly undergo a dynamic removal of their passive film (depassivation) and a repassivation. The kinetics of repassivtaion crtitically affects the corrosion-wear of such passive materials [34-37]. Different models were proposed to describe the repassivation behavior of passive materials [38-44]. Among these models, the high field ion conduction model has received most attention. A number of deviations such as Tafel slope anormalies and shape of transients (overshooting current or potential, delayed oxide formation), still have to be explained [45]. Macdonald et al. [44] analyzed the current transients and the film thickness on tungsten in a phosphate buffer solution. They showed the high-field ion conduction

model did not predict a decrease in film thickness, nor did it recognize the existence of simultaneous steady states in the film thickness and the current. Scully et al. [46] even claimed that the the high field ion conduction model was not appropriate to describe the potentiostatic repassivation of titanium in chloride solutions. Nevertheless, the high field ion conduction model has been used to predict stress corrosion susceptibility and protectiveness of passive films [47-49]. Landolt et al. [34] applied the high-field ion conduction model to investigate repassivation current transients under tribocorrosion conditions. Their numerical simulations showed that the high-field ion conduction model gives a good qualitative description of the evolution of current with the time, but important quantitative discrepancies between simulated and measured current transients remain. Indeed, the high field ion conduction model may not be physically realistic at the very short times following depassivation, but it provides a useful insight into the behaviour of oxide growth at later stages [34,45].

Most of the studies on repassivation kinetics of passive materials were performed under potentiostatic conditions. Depassivation techniques such as sliding, scratching, guillotining, potential pulse, pulsed laser and micro-tribocorrosion were used [8].

4. EXPERIMENTAL

4.1 Materials and Method

316L stainless steel provided by K.U. Leuven MTM workshop was used as test sample. Samples were machined as cilinders cut from a 316L stainless steel bar with a diameter of 20 mm and a height of 2.5 mm. Then, the specimens were ground with silicon carbide paper of 180, 320, 800, 1200 and 4000 grades followed by polishing on a rotating wheel by successively a 3 µm diamond solution, 1µm diamond solution, and 0.05 µm colloidal silica solution using a Jean Wirtz Pressair ETF 250 automatic polishing machine.

Reciprocating bidirectional (fretting) tests were performed in a ball-on-flat configuration using a microtribometer (MUST tester developed by Falex Tribology) that allows to keep the reciprocating table at a fixed position for a selected time duration during the fretting tests (Fig 4.1).

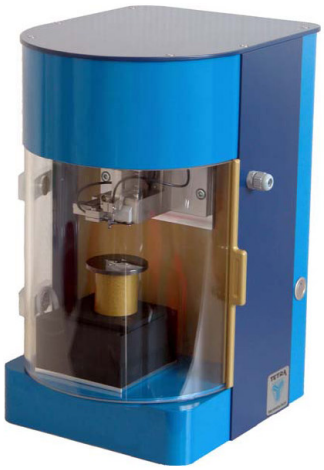

Figure 4.1: Falex Tribology MUST tester [50]

The measuring set up used for testing consists of a cantilever that have a normal stiffness value, Kn, of 0.671 mN/µm and a tangential stiffness value, Kt, of 1.237 mN/µm. The deflections in both directions of the cantilever are detected with a set of optical sensors placed in both normal and tangential direction of the cantilever (Fig 4.2). These

deflections are multiplied with the respective stiffness constants, and recorded. Depending on the range of normal forces required, a cantilever with different stiffness can be used.

The counterbody is glued at the end of this cantilever and the test sample to be tested is placed on top of the reciprocating table. After applying a normal force, the table with the sample reciprocates for a fixed displacement amplitude. By measuring the deflection of the cantilever in the tangential direction, the friction force is calculated. By measuring the cantilever deflection in the z direction, the magnitude of the applied normal force is controlled.

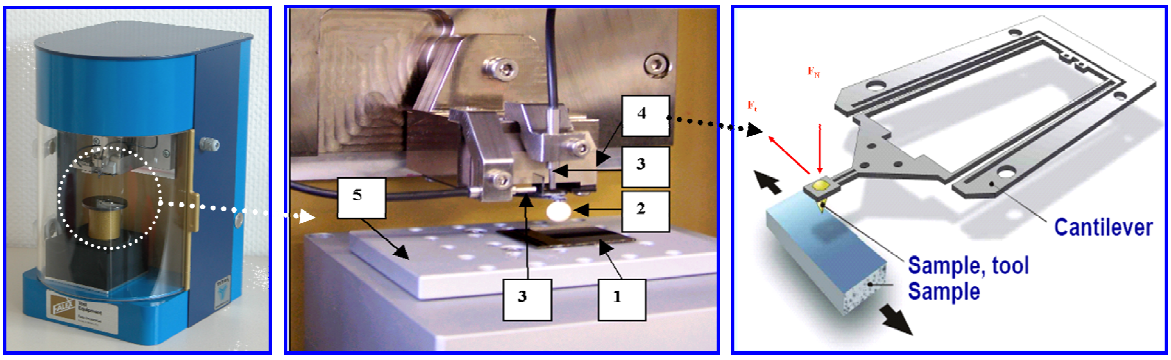

Figure 4.2: MUST microtribometer and its components.(1.test sample, 2.counterbody, 3.optical sensors, 4. cantilever, 5.reciprocating table.)

Ambient air of 23 °C and 50% RH was the test environment for all fretting tests performed under dry conditions. After polishing, samples were ultrasonically cleaned with ethanol and dried in warm air prior to the fretting tests. As a result of polishing a surface roughness of Ra=0.02 µm was obtained. The surface roughness was determined with a NT 3300 Wyko surface profilometer.

Fretting test parameters selected are given in Table 4.1. These fretting test parameters were kept constant for all fretting tests, except the holding time applied.

Table 4.1: Fretting test parameters

Parameters	**Value**
Test sample	316L SS (polished)
Counterbody	Al_2O_3(5 mm diameter)
Stroke length (peak-to-peak)	500 µm
Sliding speed	1 mm/s
Normal load	100 mN
Environment	Ambient air(23°C, % RH)
Number of cycles	400

To analyse the fretting wear behaviour of 316L stainless steel for varying exposure time of the active wear track to the ambient air, fretting tests with holding times of 0.5 s, 2 s, 4 s, 5 s, 8 s, and 10 s were carried out (named as intermittent fretting tests). Fretting test without any holding time (named as continuous fretting tests) also carried out.

Corundum balls of 5 mm diameter were loaded on top of the stainless steel samples at a normal force of 100 mN. This normal force corresponds to a maximum contact pressure of 370 mPa. A linear peak-to-peak displacement amplitude of 500 µm was applied in order to generate gross slip conditions. Prior to each fretting test, both sample and counterbody were degreased with ethanol for 60 s. All fretting tests under dry conditions were carried out at different locations on the same sample in order to avoid as much as possible different surface characteristics. All fretting tests were triplicated for the same set of testing parameters.

After each fretting test, the dissipated friction energy, the variation of dynamic frictional force, and the tangential force-displacement hysteresis loops were acquired. The average coefficient of friction value was determined based on the dissipated energy approach. The dissipated energy values (E_d) are obtained by calculating the area of each fretting loop. When E_d is the dissipated energy calculated for a particular cycle as $\int F_t \cdot dx$, with F_t the immediate tangential force, then the average coefficient of friction, µ, is given by

$$\mu = \frac{E_d}{2.d.F_n} \qquad \textbf{(4.1)}$$

with F_n the normal force, and d the net sliding distance. The net sliding distance is equal to the slip distance obtained either during forward or reverse stroke of a reciprocating sliding cycle.

4.2 Characterization Work

Wear scars formed as a result of fretting tests were analyzed by NT 3300 Wyko surface profilometer. Then fretting scars were analyzed by Scanning Electron Microscopy (SEM, Philips XL 30). The grain orientation was examined at the wear track areas generated by the fretting tests with holding times of 4 and 5 s. The reason for analyzing the grain orientation in the wear tracks generated at these holding times, will be discussed in the discussion part (see section 5.4). The examination of the grain orientation was done by using a Philips XL 30 SEM-microscope equipped with an EDAX (TSL) Orientation Image Microscopy (OIM) system.

5. RESULTS

5.1 Friction and Wear Results

The evolution of the tangential force throughout the fretting period at a given holding time, is shown in Fig. 5.1. For the continuous and intermittent fretting tests(holding time of 0.5 s. and 2 s), the tangential force increases up to a high value of approximately 75 mN, after the running-in period.

The running-in period can be considered as the period of removal of the passive oxide layer. This removal takes places more rapidly during continuous fretting tests compared to ones with holding time of 0.5 s. And during fretting tests with a holding time of 0.5 s, it takes place more rapidly compared to the ones performed at a holding time of 2 s. It was noticed that the running-in period lasts for 40 cycles in continuous fretting tests , 50 cycles in intermittent fretting tests (holding time 0.5 s), and 75 cycles in intermittent fretting tests (holding time 2,0 s).

The intermittent fretting tests (holding time of 8 and 10 s), display almost the same variation of the tangential force as a function of number of cycles. The tangential force is fluctuating around 35 mN and it is hard to define a running-in period for such tests performed at holding times of 8 and 10 s. In this case, a breakthrough of the oxide layer on top of 316L stainless steel did not occur, so that the tribocouple tested in the contact zone remained an oxide layer on 316L stainless steel and corundum from the beginning till the end of the fretting test. Hence, the tangential force stays almost constant during the test period. As a consequence, at holding times of 8 and 10 s, 316L stainless steel repassivates under the given fretting test conditions, and it keeps itself protected during the whole test period. On the contrary, during the continuous fretting tests and intermittent fretting tests with holding times of 0.5 and 2 s, 316L stainless steel can not repassivate. So the tribocouple in the sliding area remains active metal and corundum. This leads to an increase of the tangential force.

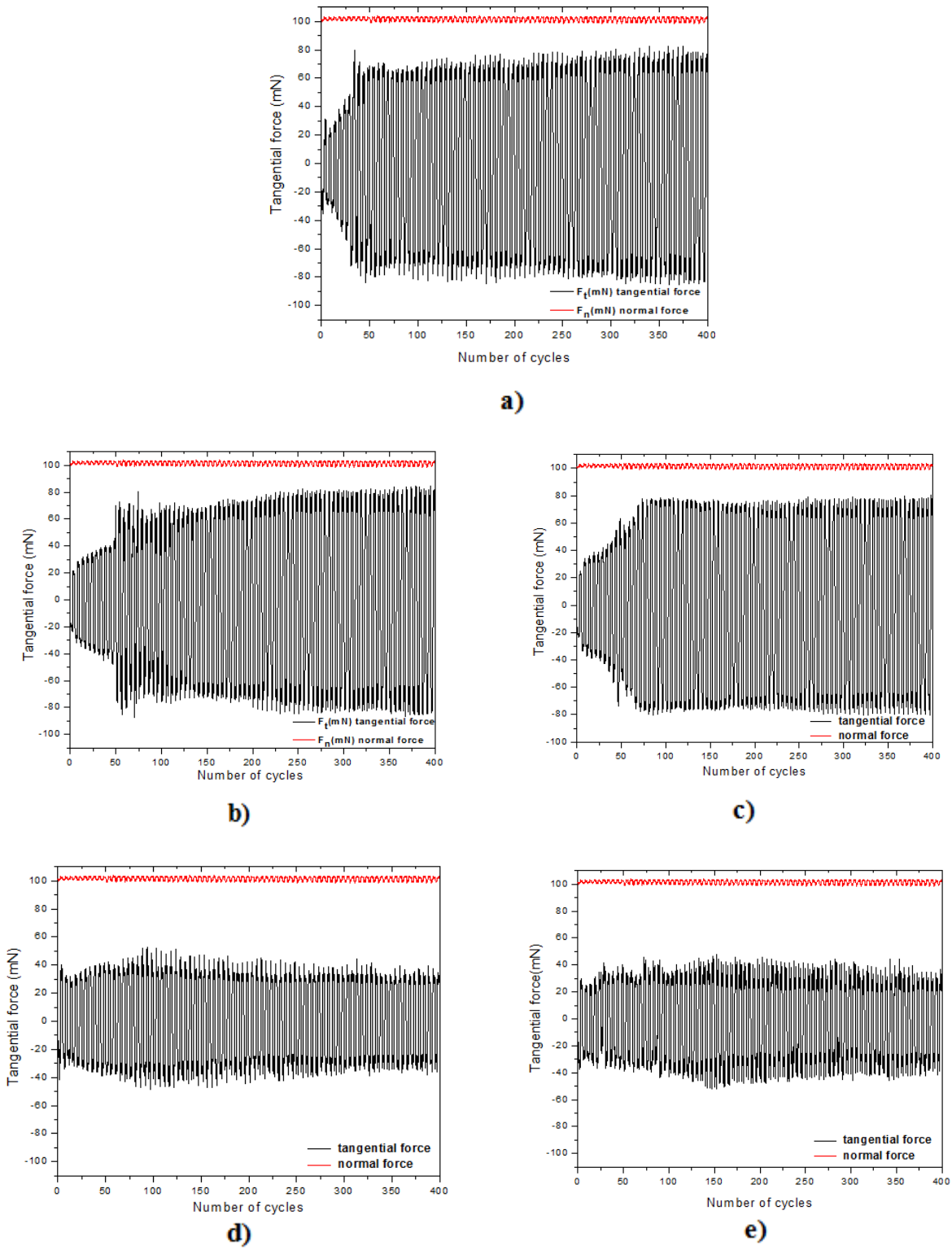

Figure 5.1: Evolution of tangential force throughout fretting period for test performed at varying holding times (a) continuous fretting, (b) intermittent fretting (holding time 0,5 s), (c) intermittent fretting (holding time 2,0 s), (d) intermittent fretting (holding time 8,0 s), (e) intermittent fretting (holding time 10,0 s)

An in-depth analysis of the coefficient of friction data brings useful insights. As it can be seen from Fig 4.2, the variation of the coefficient of friction during continuous fretting tests (no holding) and intermittent fretting tests (holding 0.5 and 2 s), differs clearly from the variation in coefficient of friction during intermittent fretting tests (8 and 10 s). The steady state coefficient of friction obtained during continuous fretting tests and intermittent fretting tests with holding time of 0.5 and 2 s, is 0.7. The coefficient of friction value obtained during intermittent fretting tests with holding time of 8 and 10 s, is 0.29. The difference in the coefficient of friction data recorded during fretting tests performed at holding times of 8 and 10 s, is quite negligible.

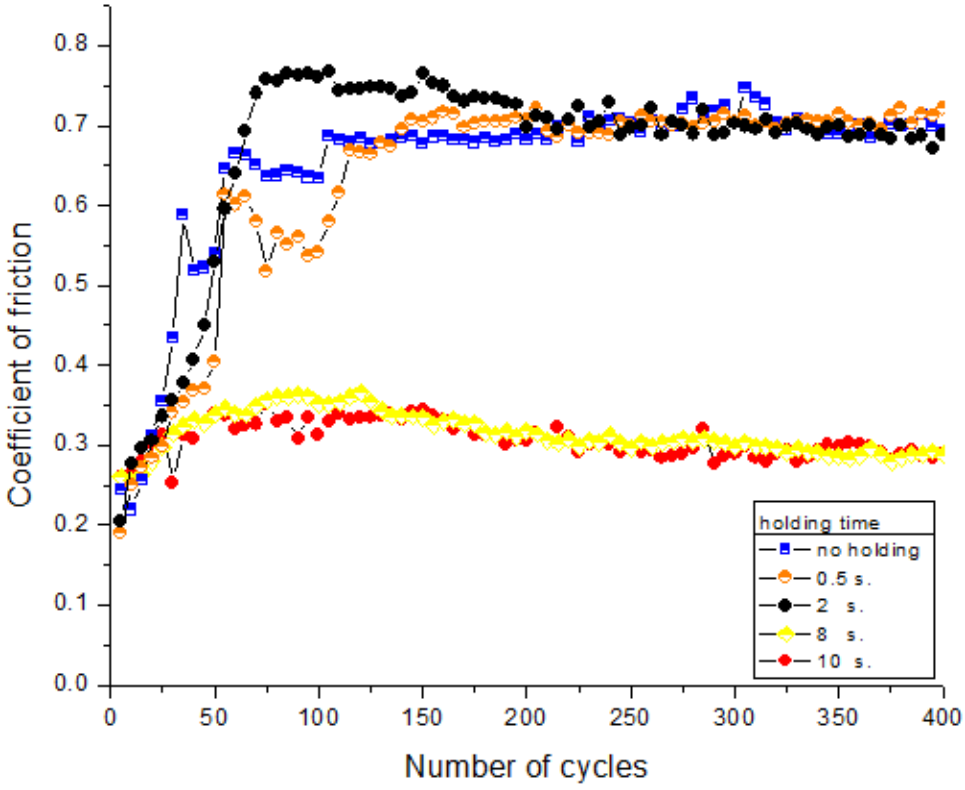

Figure 5.2: Variation of the coefficient of friction as a function of number of cycles recorded during fretting tests performed on 316L stainless steel sliding against corundum balls in ambient air of 23 °C and 50% RH. The varying test parameter was the holding time.

The coefficient of friction obtained during continuous fretting tests and intermittent fretting tests with holding times of 0.5 and 2 s, shows a fluctuation after the running-in periods. Then all stabilizes at 0.7 starting from 200th cycle.

A high coefficient of friction value was obtained during fretting tests performed at a holding time below 2 s, compared to fretting tests performed at holding times above 8 s. The main factor controlling this difference is the lubricating action of the oxide layer re-generated in the wear track depending on the exposure time which is controlled by the holding time applied.

5.2 Profilometric Analyses Results

Profilometric surface analysis of the wear scars obtained after fretting tests are shown in Table 3.4. Profilometric surface analyses results can be correlated to the coefficient of friction data. The profilometric analyses demonstrated that for wear scars resulting from intermittent fretting tests with holding time of 8 and 10 s, it is hard to detect a wear scar compared to continuous fretting tests and intermittent fretting tests with the holding times of 0.5 and 2 s. Generally speaking, fretting wear scars of continuous and intermittent fretting tests with holding times of 0.5 and 2 s are characterized by the appearance of oxide rich wear debris which are pushed to the edges and the turning points of the wear tracks.

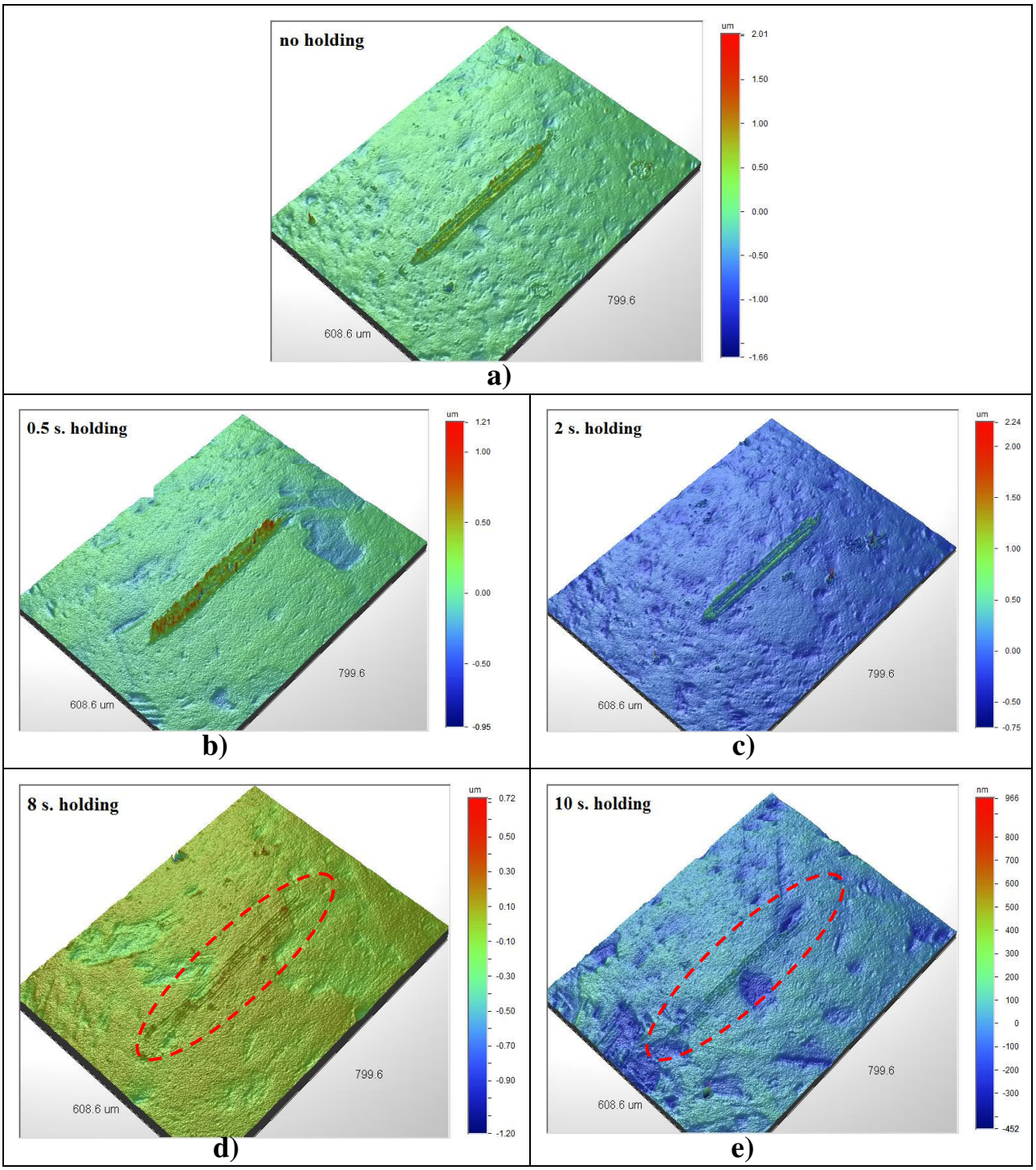

Figure 5.3: 3D profilometric surface topography of the fretting scars on 316L stainless steel obtained at different holding times in ambient air test conditions (a) continuous fretting, (b) intermittent fretting (holding time 0,5 s), (c) intermittent fretting (holding time 2,0 s), (d) intermittent fretting (holding time 8,0 s), (e) intermittent fretting (holding time 10,0 s)

Due to the limited wear volume, wear depth data were smoothen by the use of a special software of Wyko NT3300. As a result of the data smoothing treatment, the surface topography of and around the fretting scars was acquired as shown in Fig. 5.4.

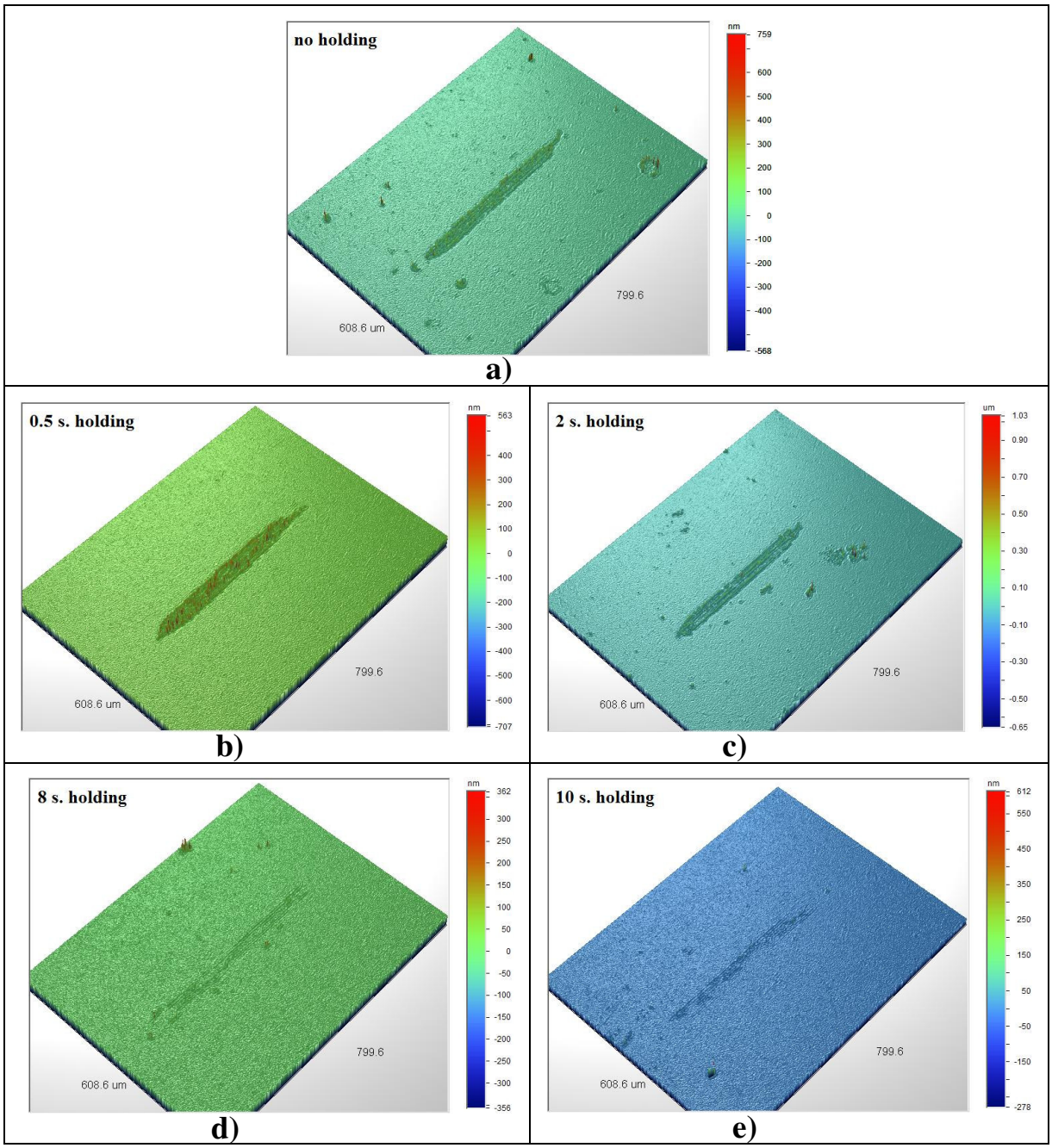

Figure 5.4: 3D surface topography of the fretting scars after smoothing treatment (a) continuous fretting, (b) intermittent fretting (holding time 0,5 s), (c) intermittent fretting (holding time 2,0 s), (d) intermittent fretting (holding time 8,0 s), (e) intermittent fretting (holding time 10,0 s)

This treatment was done to obtain comparative results about the depths of the wear tracks generated during fretting tests performed at varying holding time. That variation of the wear depth of fretting scars is given in Fig 5.5. The measurement of the wear depths of each fretting scar was done in the middle of the fretting track scanning from left to right perpendicular to the sliding direction.

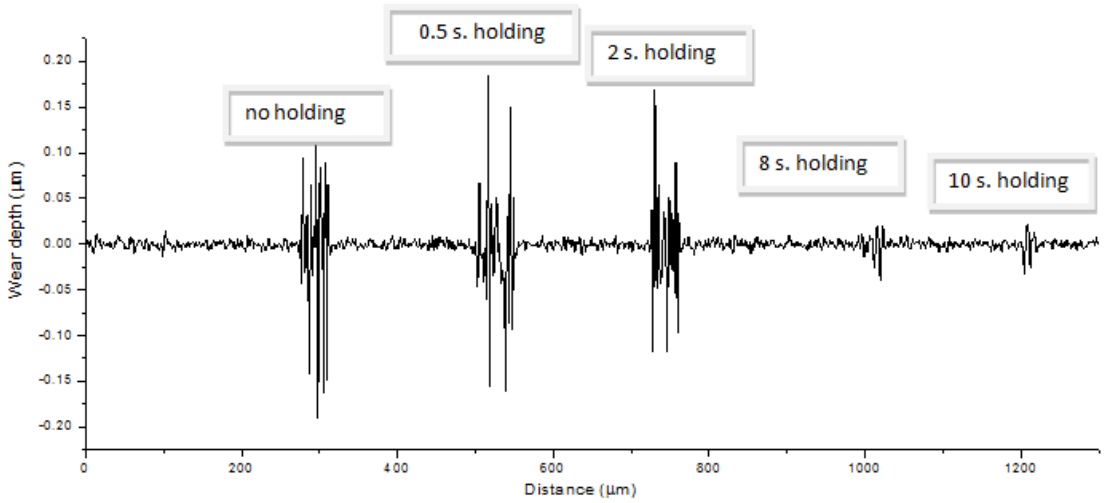

Figure 5.5: Variation of the depth of wear scars on 316L stainless steel obtained after fretting tests done at different holding times in ambient air of 50% RH

Compared to the continuous fretting tests (no holding) and intermittent fretting tests with holding times of 0.5 and 2 s, a very small and narrow variation of wear track depth was noticed after intermittent fretting tests performed at a holding time of 8 and 10 s.

5.3 Scanning Electron Microscope (SEM) Analyses Results

SEM images of the wear tracks indicate that continuous fretting tests and intermittent fretting tests with holding times of 0.5 and 2 s generated quite deep wear scars compared to fretting tests performed at holding times of 8 and 10 s. Fretting wear scars generated as a result of continuous fretting tests and intermittent fretting tests with holding times of 0.5 and 2 s exhibit regular continuous abrasive scratches that are generated by the continuous removal of the oxide layer during the sliding periods, since there is no remarkable wear appearing as a result of intermittent fretting tests with holding time of 8 and 10 s. In Figures 5.6 and 5.7 SEM images of the wear scars resulted by intermittent fretting tests with holding time of 2 and 8 s. are shown comparatively.

Additionally, in the middle of the wear scars of the continuous fretting tests performed and with a holding time of 0.5 s, oxide rich particles (debris) are observed throughout the wear tracks (see appendix). In the wear tracks, plastic deformation of 316L stainless steel might have occurred and removed oxide particles during the fretting might have accumulated. That may contribute to the generation of the wear debris in the middle of the wear tracks as seen on the variation of the wear depths in Fig 5.5.

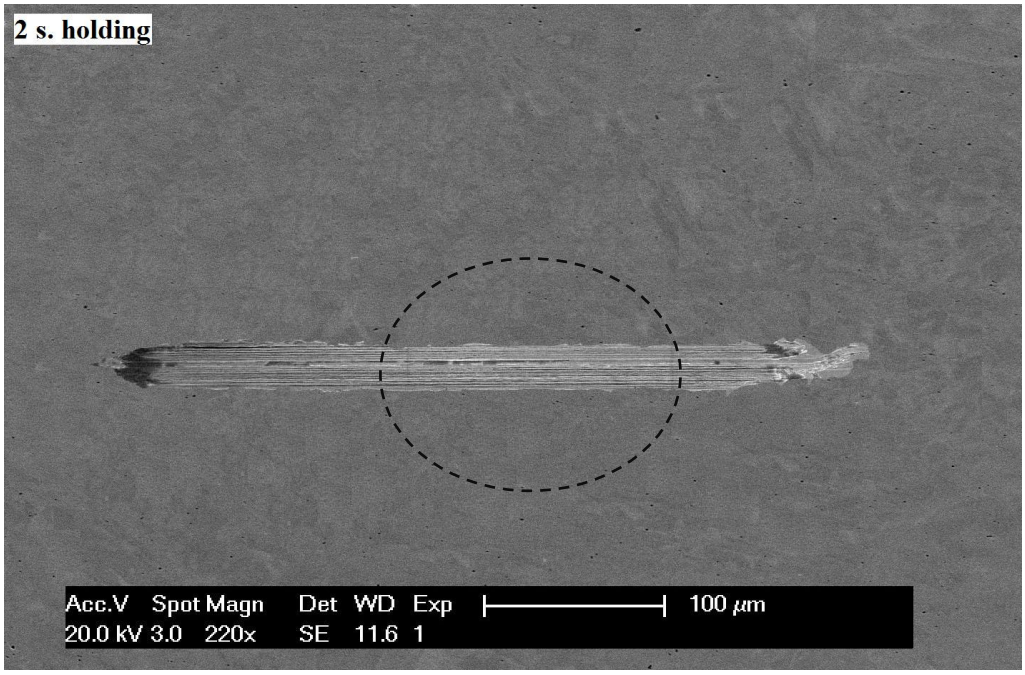

a)

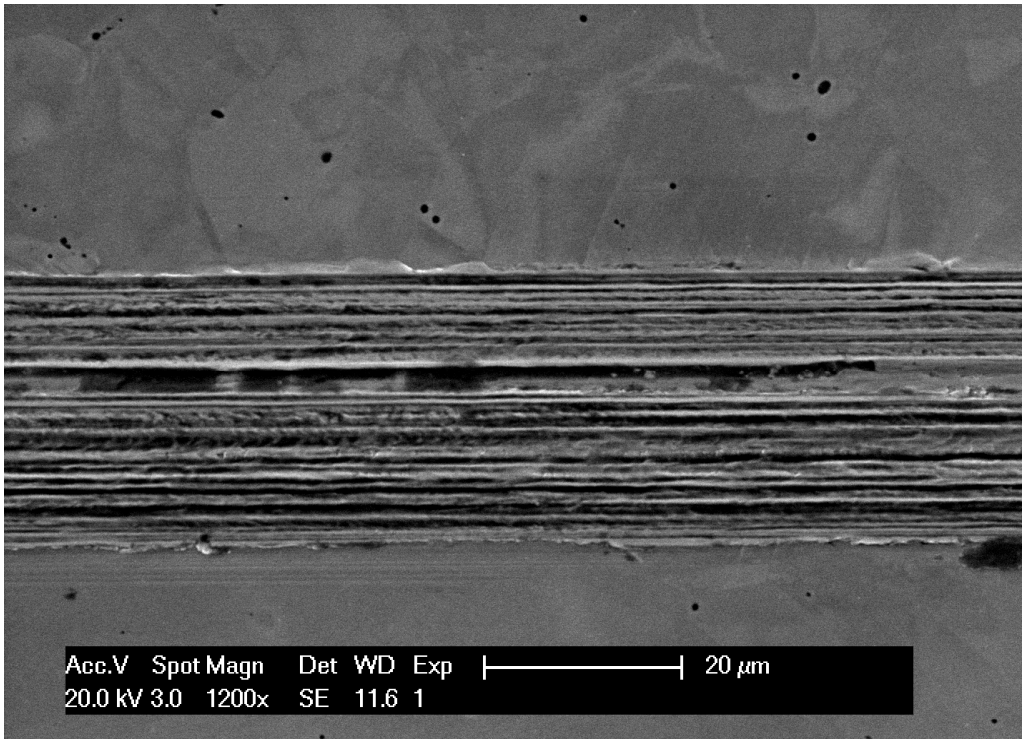

b)

Figure 5.6: SEM images of fretting scars a) SEM of fretting scar on 316L stainless steel obtained after a fretting test performed at a holding time of 2 s for 400 cycles, b) a zoom-in view of circled area

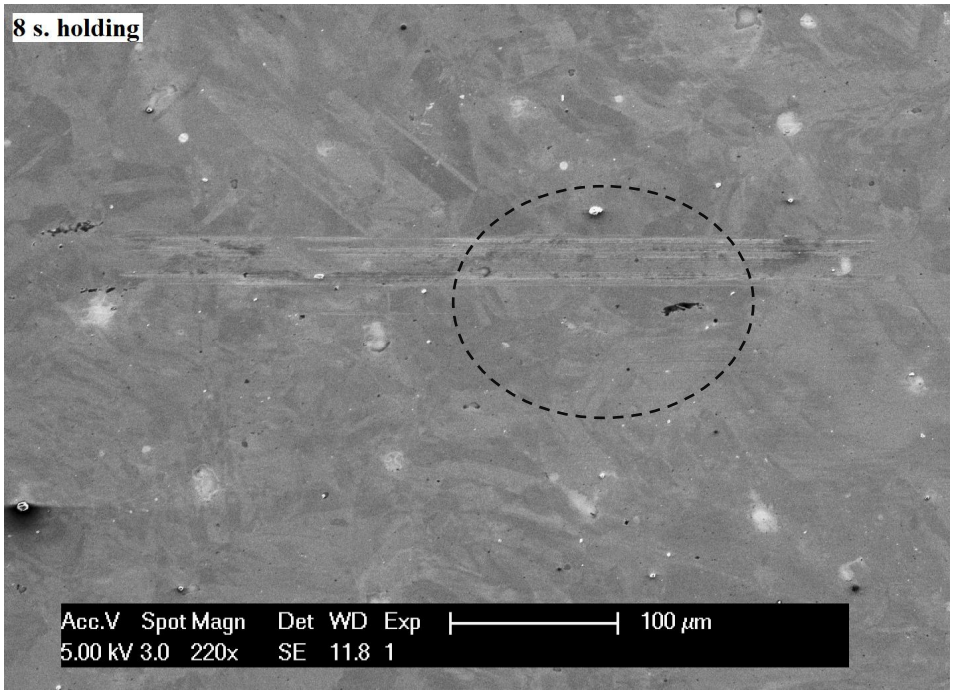

a)

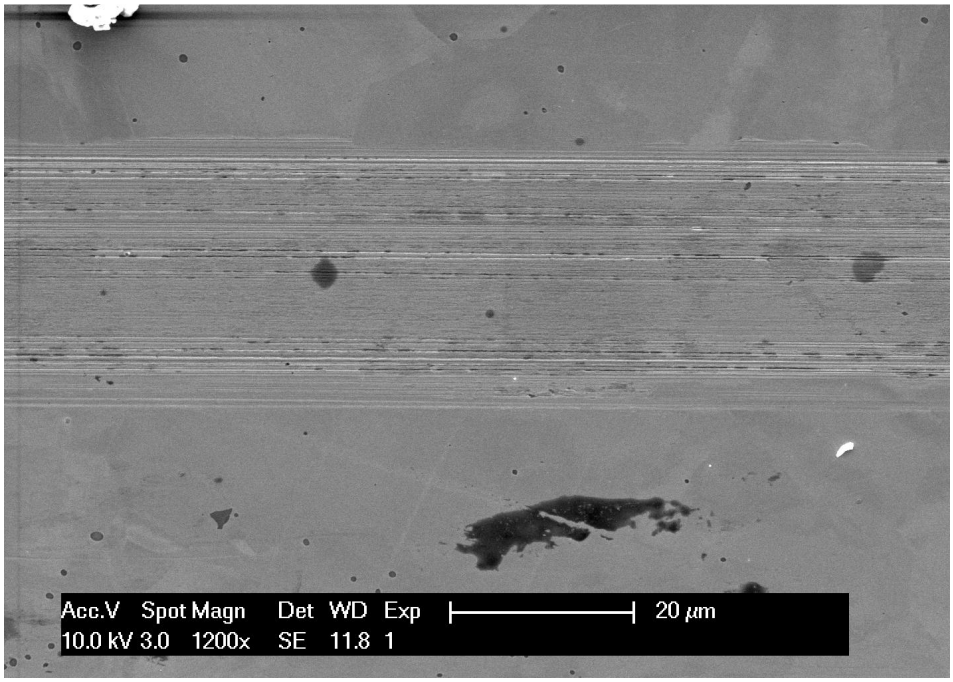

b)

Figure 5.7: SEM of fretting scar obtained by the intermittent fretting test with holding time of 8 s and its zoom in view a) SEM of fretting scar on 316L stainless steel obtained after a fretting test performed at a holding time of 8 s for 400 cycles, b) a zoom-in view of circled area

5.4 Orientation Image Microscopy (OIM) Analyses Results

The aim of the OIM studies was to evaluate the limited repeatability of the fretting tests conducted for intermittent fretting tests for holding times 4 and 5 s. Thus, during the course of this research some of the experimental results of the fretting tests performed at holding times of 4 and 5 s did not match with the results of fretting test performed under identical test conditions on the same sample.

In general a high coefficient of friction ranging from 0.69 to 0.66 was recorded during fretting tests performed at a holding time of 4 s. However, sometimes coefficient of friction of 0.29 was obtained from during repeated tests. In the same respect, a high coefficient of friction of 0.63 was recorded in general during fretting tests performed at a holding time of 5 s, sometimes a low coefficient of friction of 0.31 was obtained from identical duplicated tests. In order to acquire an insight on this variation, the grain orientation was analyzed at areas containing the wear track of the fretting tests performed at holding times of 4 and 5 s (Fig 5.8).

From the Orientation Image Microscopy (OIM) scans, an average grain size of 50 µm was obtained. Additionally, no remarkable difference in the grain size distribution and no preferential grain orientation were determined at areas on 316L stainless steel sample where fretting wear scars generated at holding times of 4 and 5 s are located.

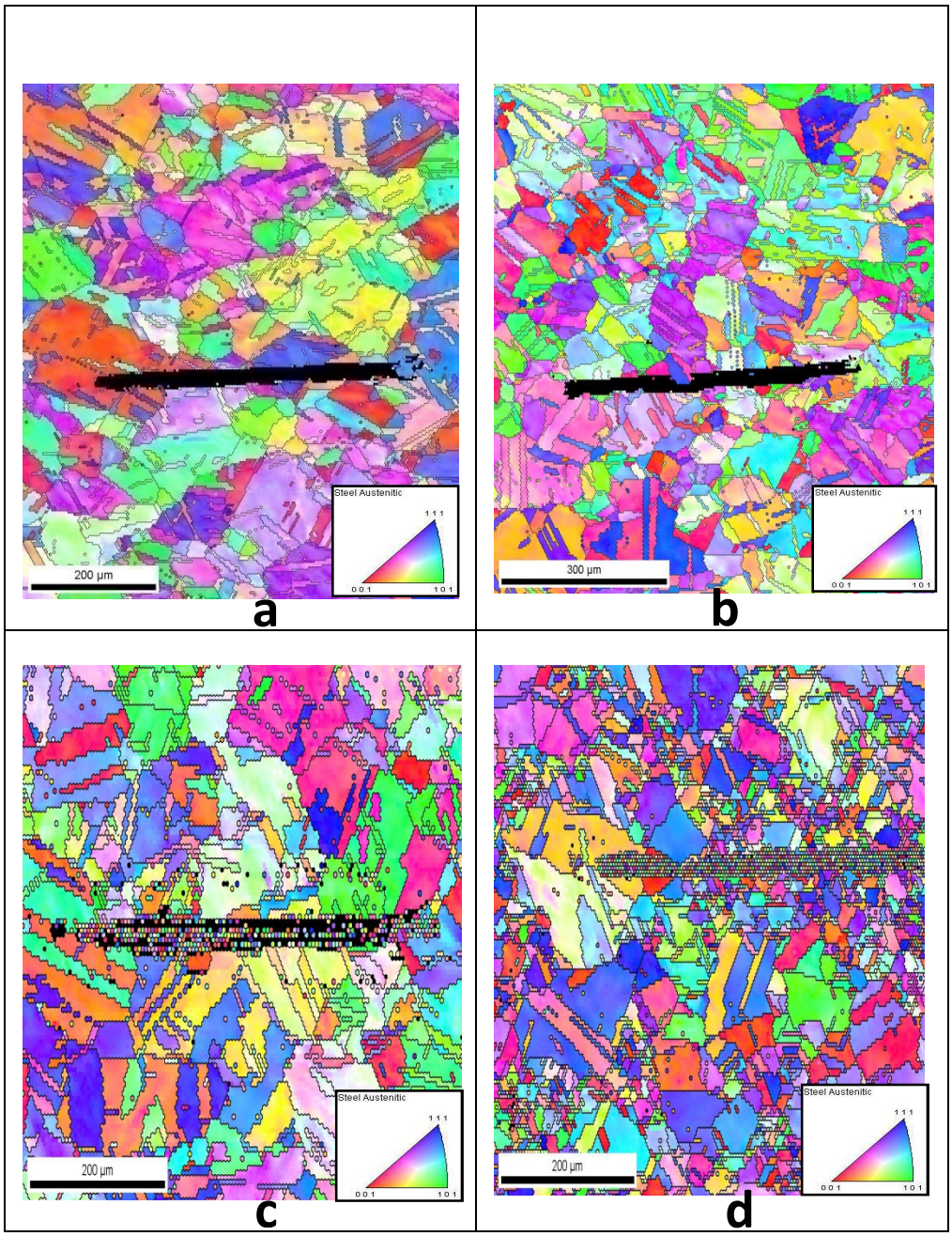

Figure 5.8: Orientation Image Microscopy (OIM) scans of the fretting scars: a) wear scar of the fretting test at a holding time of 4 s during which an average coefficient of friction of 0.69 was recorded, b) wear scar of the fretting test at a holding time of 4 s during which an average coefficient of friction of 0.29 was recorded, c) wear scar of the fretting test at a holding time of 5 s during which an average coefficient of friction of 0.63 was obtained, and d) wear scar of the fretting test at a holding time of 5 s during which an average coefficient of friction of 0.31 was obtained.

6. DISCUSSION

The main factor causing either a high coefficient of friction of 0.7 approx. or a low coefficient of friction of 0.29 approx., is the passive oxide layer that regenerates in the wear track in between successive sliding events. A high coefficient of friction of 0.7 was obtained during fretting tests performed at a holding time below 2 s, while on the contrary a low coefficient of friction of 0.29 was noticed during fretting tests performed at a holding time above 8 s. The holding times of 4 and 5 s may correspond to the transition time at which the regeneration of the oxide layer on 316L stainless steel takes place. And this may be the reason why non-identical coefficients of friction were noticed during fretting tests performed at holding times of 4 and 5 s. Working under conditions where a transition in surface reaction takes place, makes the process more sensitive to minor differences in external test conditions.

Exposure time of the active wear track to the ambient air during the sliding, critically affects the evolution of the friction and wear. Depending on the exposure time of the active wear track to the ambient air, bare surface heal (repassivates) itself or leads to removal and degradation. The time period required for repassivation gives a very useful insight on repassivation kinetics. As a results of the work, it's been determined that repassivation of the 316L under reciprocating sliding contacts occurs in between 2 and 8 s in the ambient air of %50 RH and 23 °C.

When all the coefficient of friction data obtained during the fretting tests are plotted as a function of holding time applied, a graph as shown in Fig 6.1 is obtained.

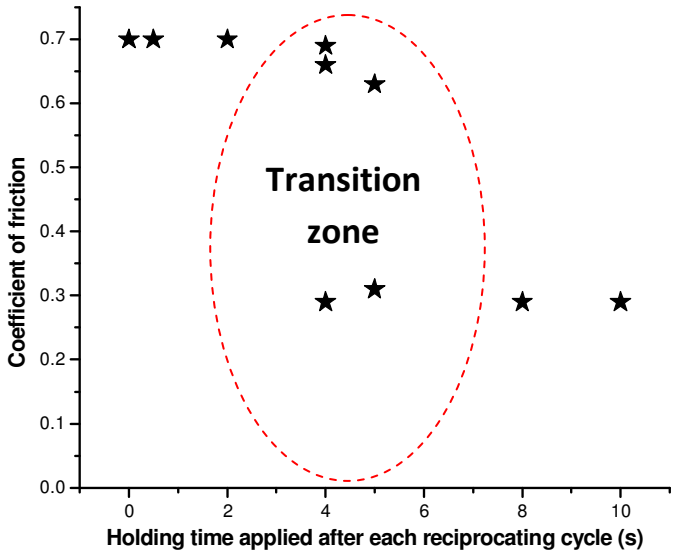

Figure 6.1: Variation of coefficient of friction as a function of holding time for fretting tests performed on 316L stainless steel sliding against corundum balls in ambient air of 50% RH.

7. CONCLUSIONS

The main conclusions that can be drawn in consequence of this study concerning with the repassivation-depassivation kinetics under reciprocating contacts are like following

1. Passive materials may easily loose their protective surface film either by wear or scratching. And this can be followed by local dissolution or repassivation depending on the loading conditions, material-environment system. Repassivation kinetics of such passive materials critically affects the wear-corrosion system.
2. At holding times of 8 and 10 s, 316L stainless steel repassivates under the given fretting test conditions, and it keeps itself protected during the whole test period. On the contrary, during the continuous fretting tests and intermittent fretting tests with holding times of 0.5 and 2 s, 316L stainless steel can not repassivate. So the tribocouple in the sliding area remains active metal and corundum. This leads to an increase of the tangential force.
3. A high coefficient of friction value was obtained during fretting tests performed at a holding time below 2 s, compared to fretting tests performed at holding times above 8 s. The main factor controlling this difference is the lubricating action of the oxide layer re-generated in the wear track depending on the exposure time which is controlled by the holding time applied.
4. Fretting wear scars of continuous and intermittent fretting tests with holding times of 0.5 and 2 s are characterized by the appearance of oxide rich wear debris which are pushed to the edges and the turning points of the wear tracks.
5. Compared to the continuous fretting tests (no holding) and intermittent fretting tests with holding times of 0.5 and 2 s, a very small and narrow variation of wear track depth was noticed after intermittent fretting tests performed at a holding time of 8 and 10 s.

6. Fretting wear scars generated as a result of continuous fretting tests and intermittent fretting tests with holding times of 0.5 and 2 s exhibit regular continuous abrasive scratches that are generated by the continuous removal of the oxide layer during the sliding periods, since there is no remarkable wear appearing as a result of intermittent fretting tests with holding time of 8 and 10 s.

REFERENCES

[1] **Watson, S.M. Friedersdorf, Madsen, F.J., B.W., and Cramer**, **S.D.,** 1995. Methods of measuring wear-corrosion synergism, *Wear,* **476**, 181–183

[2] **Mischler S., in: Zambelli G., and Vincent, L.,** 1998. Mate´riaux et Contacts, *PPUR Chap. 9, Lausanne*, 107.

[3] **Robert, J., and Wood, K.**, 2007. Tribocorrosion of coatings: a review, *Applied Physics*, **40**, 5502-5521.

[4] **Fontana, M.G**., 1986. Corrosion Engineering, McGraw-Hill Book, New York.

[5] **Berradja, A., Bratu, F., Benea, L., Willems, G., and Celis, J.-P**., 2006. Effect of sliding wear on tribocorrosion behaviour of stainless steels in a Ringer's solution, *Wear,* **261,** 987–993.

[6] **Pei-Qiang, W., and Celis, J.-P.,** 2004. Ion conduction model applied to repassivation kinetics of tribo-activated surfaces, *Journal of the Electrochemical Society*, **151,** 551-557.

[7] **Landolt, D. Mischler, S., and Stemp, M.,** 2001. Electrochemical methods in tribocorrosion: A critical appraisal, *Electrochimica Acta*, **46**, 3913-3929.

[8] **Pei-Qiang, W.,** 2003. Triboelectrochemical investigation of fretting corrosion, *PhD dissertation*, KU Leuven, Belgium

[9] **Williems, G., Clocheret, K., Celis, J.P., Verbeke, G., and Chatzicharalampous Carels, E. C.,** 2001. Frictional Behaviour of Stainless Steel Bracket-Wire Combinations subjected to Small Oscillating Displacements, *American J. Orthodontics and Dentofacial Orthopedics*, **120**, 371-377.

[10] **Mohrbaecker, H.,** 1995. The tribological performance of advanced hard coatings under fretting conditions, *PhD dissertation*, KU Leuven, Belgium

[11] **Tritschler, B., Forest, B., and Rieu, J.,** 1999. Fretting corrosion of materials for orthopaedic implants: a study of a metal/polymer contact in an artificial physiological medium, *Tribology International*, **32***,* 587-596.

[12] **Waterhouse, R.B.,** 1981. Materials Evaluation under Fretting Conditions, ed. S.R. Brown, Philadelphia.

[13] **Waterhouse, R.B.,** 1992. ASM Handbook, Vol. 18, ASM International, Ohio, USA.

[14] **Waterhouse, R.B.,** 1992. Fretting Fatigue, *Int. Mat. Rev.*, **37**, 77-97.

[15] **Mohrbacher, H., Blanpain, B., Celis, J.P., and Roos, J.R.,** 1995. The influence of humidity on the fretting behaviour of PVD TiN coatings, *Wear,* **180,** 43-44.

[16] **Mischler, S., Debaud, S., and Landolt, D.,** 1998. Wear-accelerated corrosion of passive metals in tribocorrosion systems, *Journal of Electrochemical Society*, **145**, 750-758.

[17] **Ponthiaux, P., Wenger, F., Drees, D., and Celis, J.P.,** 2004. Electrochemical techniques for studying tribocorrosion processes, *Wear,* **256**, 459–468.

[18] **Oltra, R., Chapey, B., and Renaud, L.,** 1995. Abrasion-Corrosion Studies of Passive Stainless Steel in Acidic Media:Combination of Acoustic Emission and Electrochemical Techniques, *Wear,* **533**, 186–187.

[19] **Schmutz, P., and Frankel, G.S.,** 1999. Influence of Dichromate Ions on Corrosion of Pure Aluminum and AA2024-T3 in NaCl Solution Studied by AFM Scratching, *Journal of Electrochemical Society,* **146,** 4461-4472.

[20] **Rabinowitz, E.,** 1965. Friction and Wear of Materials, Wiley, New York.

[21] **Lim, S.C., and Ashby, M.F.,** 1987. Wear-mechanism maps, *Acta Met.* **35**, 1-24.

[22] **Quinn, T.F.J., Sullivan, J.L., and Rowson, D.M.,** 1984. Origins and development of oxidational wear at low ambient temperatures, *Wear,* **94,** 175-191.

[23] **Stott, F.H.,** 1998. The role of oxidation in the wear of alloys, *Tribol. Int.* **31**, 61-71.

[24] **Waterhouse, R.B.,** 1972. Fretting Corrosion, Pergamon Press, Oxford.

[25] **Brandon, N.P., Bonanos, N., Fogarty, P.O., and Mamoud, M.N.**, 1992. The Effect of Interfacial Potential on Friction in a Model Aqueous Lubricant, *J. Electrochem. Soc*. 139, 3489-3492.

[26] **Hong, M.H., and Pyun, S.I.,** 1991. Corrosive wear behaviour of 304-L stainless in 1 N H_2SO_4 solution: Part 1. Effect of applied potential, *Wear,* **147,** 59-67.

[27] **Iwabuchi, A., Tsukamoto, T., Shimizu, T., and Yasiro, H.,** 1998. The Mechanism Of Corrosive Wear Of An Austenitic Stainless Steel In An Aqueous Electrolyte Solution, *Tribol. Trans.*, **41**, 96-102.

[28] **Iwabuchi, A., Tsukamoto, T., and Tatsuyanagi, T.Y.,** 1992. Electrochemical approach to corrosive wear of SKD61 die steel in Na_2SO_4 solution, *Wear,* **156**, 301-313.

[29] **Abd-el-Kader, H., and El-Raghy, S.M.,** 1986. Wear-corrosion mechanism of stainless steel in chloride media, *Corros. Sci.,* **26**, 647-653.

[30] **Abd-el-Kader, H., and El-Raghy, S.M.,** 1985. Electrochemical kinetics of stainless steel in aerated chloride solutions during wear process, *Electrochim Acta,* **30**, 841-842.

[31] **Xiaoxia, J., Shizhuo, L., Chengtian, D., and Ming, L.,** 1989. Study of the Corrosive Wear of Ti-6Al-4V in Acidic Medium, *Wear,* **129**, 293-294.

[32] **Adler, T.A., and Walters, R.P.,** 1992. Corrosion and wear of 304 stainless steel using a scratch test, *Corros. Sci.* **33**, 1855-1876.

[33] **Mischler, S., Debaud, S., and Landolt, D.,** 1998. Wear-accelerated corrosion of passive metals in tribocorrosion systems, *J. Electrochem. Soc.,* **145**, 750-758.

[34] **Jemmely, P., Mischler, S., and Landolt, D.,** 2000. Electrochemical modeling of passivation phenomena in tribocorrosion, *Wear,* **237**, 63-76.

[35] **Madsen, B.W., and Adler, T.A.,** 1994. Passivation and repassivation kinetics of iron-aluminum alloys in 1 N H_2SO_4 using potential step and scratch tests, *Wear,* **171**, 215-225.

[36] **Garcia, I., Drees, D. and Celis, J.P.,** 2001. Corrosion-wear of passivating materials in sliding contacts based onj a concept of active wear track area, *Wear*, **249**, 452-460.

[37] **Iwabuchi, A., Sonoda, T., Yashiro, H. and Shimizu, T.,** 1999. Application of potential pulse method to the corrosion behaviour of the fresh surface formed by scratching and sliding in corrosive wear, *Wear*, **225-229**, 181-189.

[38] **Ratzer-Scheibe, H. J.,** 1983. Repassivation of titanium and titanium alloys dependent on potential and PH in *Passivity of Metals and Semiconductors*, pp.731-739, Elsevier Science Publications, Amsterdam.

[39] **Burstein, G. T. and Marshall, P. I.,** 1983. Growth of Passivating Films on Scratched 304L Stainless Steel in Alkaline Solution, *Corrosion Science*, **23**, 125-137.

[40] **Barbosa, M.,** 1988. A model for the kinetics of repassivation II: scratching electrodes, *Corrosion*, **44**, 149-153.

[41] **Adler, T. A., and Walters, R. P.,** 1993. Repassivation of 304 stainless steel investigated with a single scratch test, *Corrosion*, **49**, 399-408.

[42] **Itagaki, M., Oltra R., Vuillemin, B., Keddam, M., and Takenouti, H.,** 1997. Quantitative analysis of iron dissolution during repassivation of freshly generated metallic surfaces, *J. Electrochem. Soc.,* **144**, 64-72.

[43] **Olsson, C. O. A., Hamm, D. and Landolt, D.,** 2000. Evolution of passive film growth models with the electrochemical quartz crystal microbalance on PVD deposited Cr, *J. Electrochem. Soc.,* **147**, 4093-4102.

[44] **Macdonald, D. D., Riafaie, M. A. and Engelhardt, G. R.,** 2001. New rate laws for the growth and reduction ofpassive films, *J. Electrochem. Soc.,* **148**, 343-347.

[45] **Lohrengel, M. M.,** 1993. Thin anodic oxide layers on aluminum and other valve metals: high field regime, *Materials Science and Engineering R*, **11**, 243-294.

[46] **Kolman, D. G., and Scully, J. R.,** 1995. Limitations of potentiostatic repassivation techniques and their relationship to the applicability of the high-field approximation to the repassivation of titanium, *J. Electrochem. Soc.,* **142,** 2179-2188.

[47] **Kwon, H. S., Cho, E. A. and Yeom, K. A.**, 2000. Prediction of stress corrosion cracking susceptibility of stainless steel based on repassivation kinetics, *Corrosion*, **56**, 32-40.

[48] **Cho, E. A., Kim, C. K., Kim, J. S. and Kwon, H. S.,** 2000. Quantitative analysis of repassivation kinetics of ferritic stainless steel based on the high field ion conduction model, *Electroc. Acta*, **45**, 1933-1942.

[49] **Li D., Mao, X. and Zhu, R.,** 1993. Kinetics of Passive Film Formation on Scratched Bare Surfaces of Stainless steels in Magnesium-Chloride Solutions, *Corrosion*, **49**, 877-884.

[50] Falex Tribology NV Homepage,

www.falexint.com, 05.05.2008.

APPENDIX A

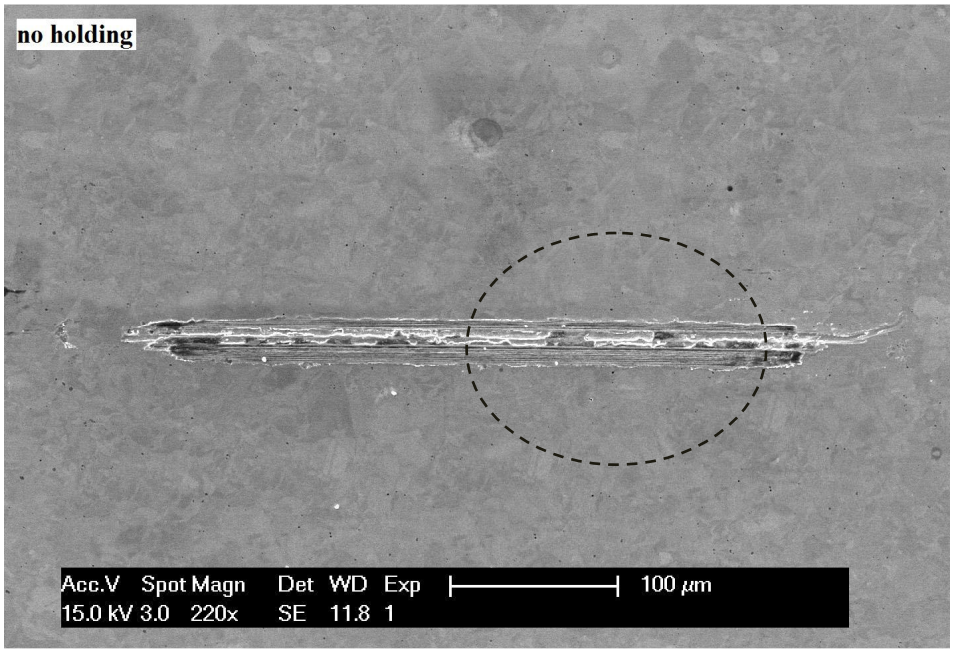

a)

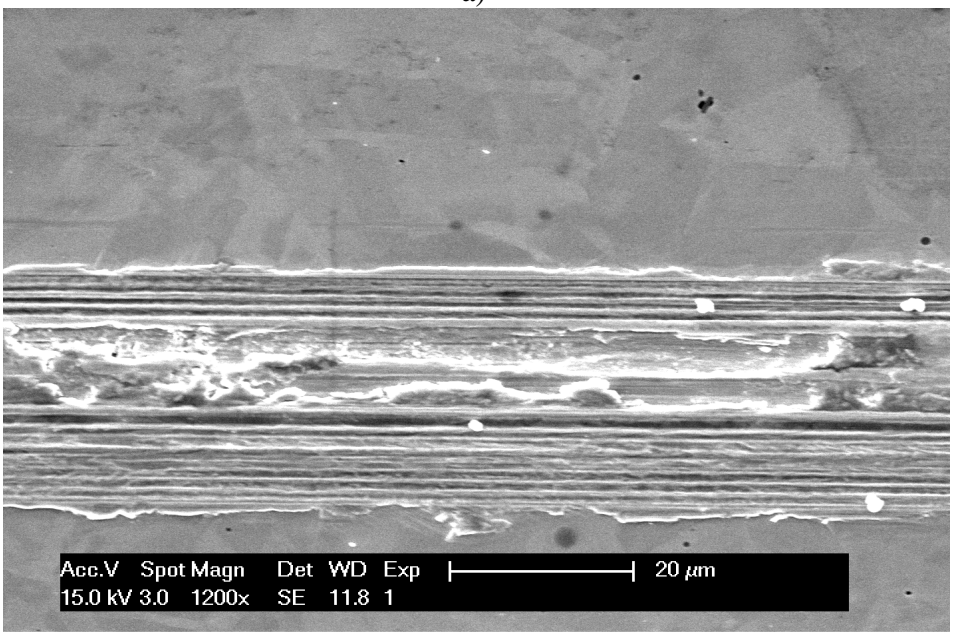

b)

Figure A.1 : Figure A.2 SEM of fretting scar obtained by the continuous fretting test and its zoom in view a) SEM of fretting scar on 316L stainless steel obtained after continuous fretting test (no holding) for 400 cycles, b) a zoom-in view of circled area

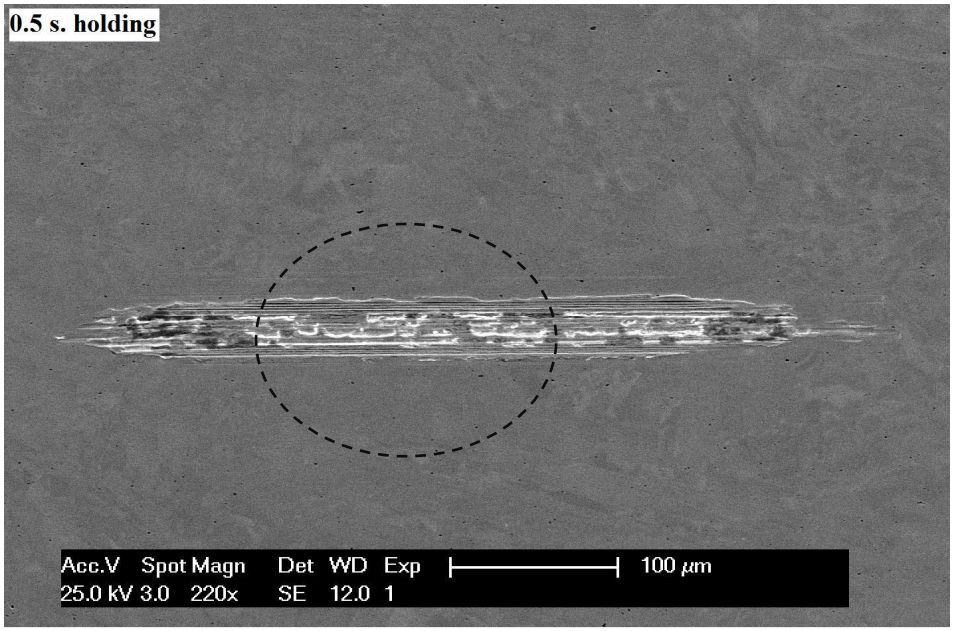

a)

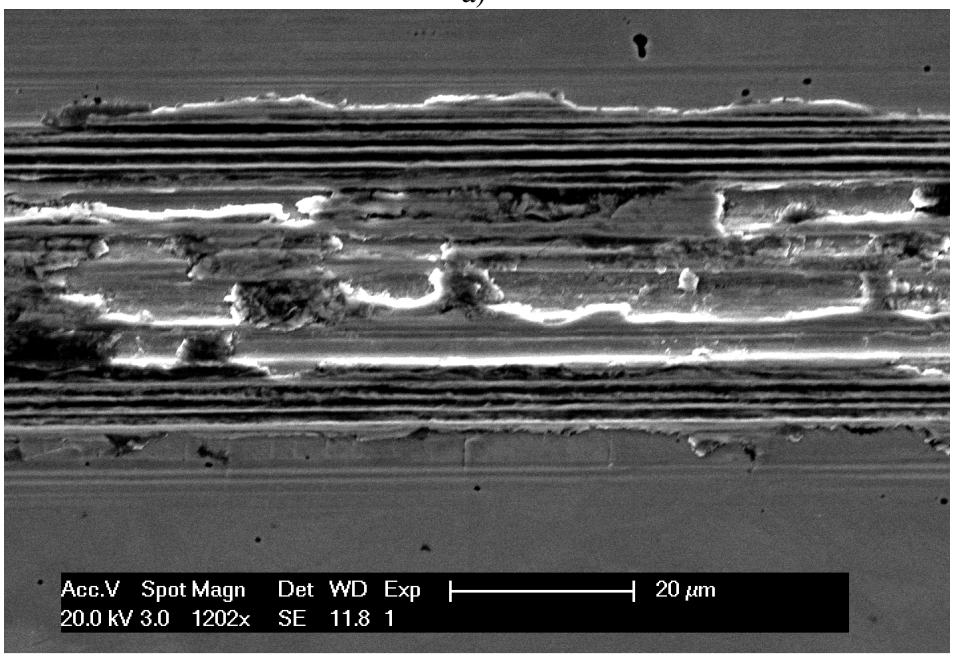

b)

Figure A.2: SEM of fretting scar obtained by the intermittent fretting test with holding time of 0.5 s and its zoom in view a) SEM of fretting scar on 316L stainless steel obtained after a fretting test performed at a holding time of 0.5 s for 400 cycles, b) a zoom-in view of circled area

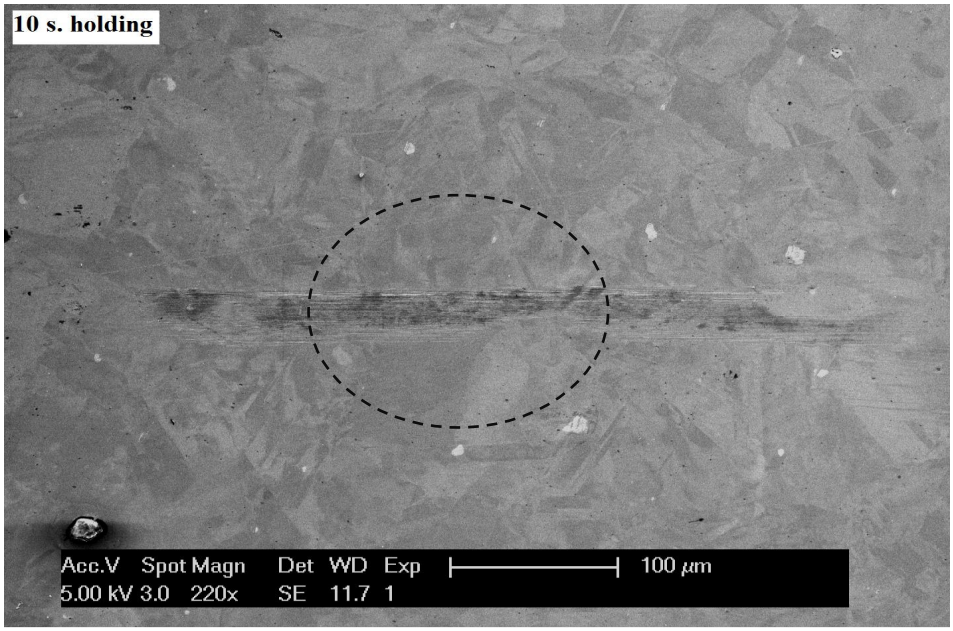

a)

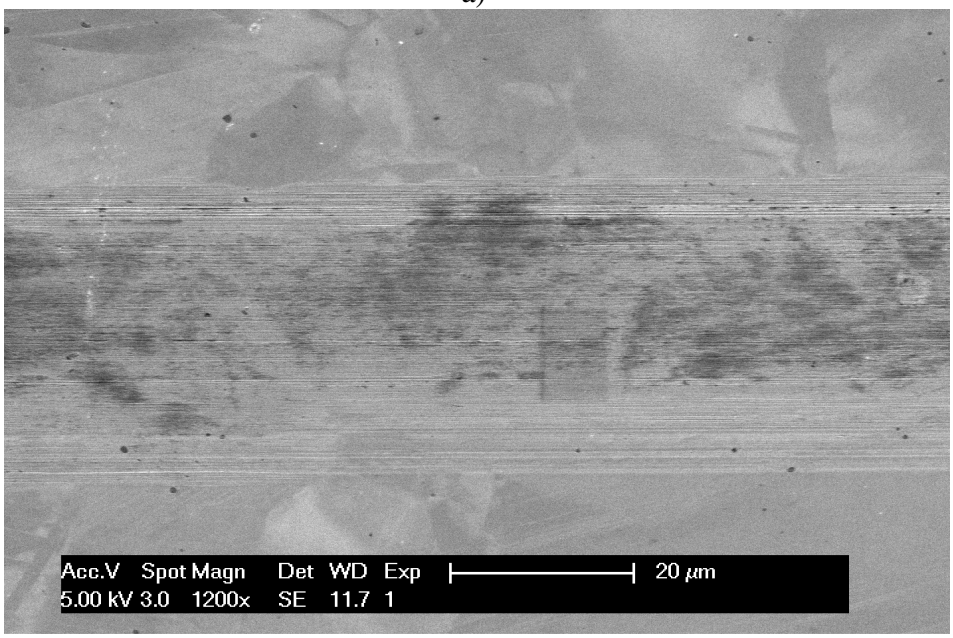

b)

Figure A.3: SEM of fretting scar obtained by the intermittent fretting test with holding time of 10 s and its zoom in view . a) SEM of fretting scar on 316L stainless steel obtained after a fretting test performed at a holding time of 10 s for 400 cycles, b) a zoom-in view of circled area

BIOGRAPHY

Gökhan BÜYÜKSARI was born in August, 23 1984 in Adapazarı. After the Marmara earthquake happened in 19th August 1999, he moved to Eskisehir. And he went on his education life in Eskisehir. He was graduated from Eskisehir Fatih Anatolian High School in 2002. Following his high school graduation from high school, he attended to Sakarya University Metallurgical and Materials Engineering in the same year. He got his degree as Bachelor's in 2006 from Sakarya University Metallurgical and Materials Engineering Department. Then he continued his career in Istanbul Technical University as a master student in the Materials Engineering program.